Document Title: Weapons And Non-permitted Devices Detector (WANDD)

Author: Luna Innovations Incorporated

Document No.: 228732

Date Received: November 2009

Award Number: 2006-IJ-CX-K023

Weapons And Non-permitted Devices Detector (WANDD)

Luna Innovations Incorporated
Grant # 2006-IJ-CX-K023
Final Report

July 31, 2008

Table of Contents

I. Executive Discussion

Luna Innovations Incorporated was awarded a grant from NIJ to develop and test a new concept for a "Weapons And Non-permitted Devices Detector (WANDD)" (*Grant # 2006-IJ-CX-K023).* The device is based on a Luna patent for an ultrasonic nonlinear system that beams focused ultrasonic energy to a small region on a person. What is unique about this device is that it converts the ultrasonic energy to lower frequencies to penetrate clothing yet remains focused within the ultrasonic envelope. The goal of the project was to test this device for corrections applications in an actual prison setting and demonstrate its ability do detect both metal and plastic contraband. The primary goals have been accomplished with safe tests at a prison, and the technology has matured to a higher readiness level. The audible sound pressure levels used are well under OSHA 1910.95 standards (<140 dB for impulse sound) and are perceived audibly as a slight chirp. The work is ready for the next phase to eliminate the umbilical cables, improve the form-factor and continue to improve the false-calls ratio.

The greatest challenge in this project was to design an approach that can be cost effective, use multi-modes of detection and detect both metal and plastics. Our design couples two modes of weapons detection in one device with one of the modes being a new approach to detect both metal and plastic devices. Luna developed an ultrasonic array, the electronic drivers for nonlinear generation, the detection and processing system and the integration of two modes into one hand held device.

Many tests were run at Luna to develop, evaluate and improve the hardware and detection extraction software. Receiver Operating Characteristics (ROC) tests show that the system is able to detect both metal and plastic devices, including plastic knives, wadded money, pen pikes and guns. We have also tested cell phones, cigarette lighters, candy sticks, keys and other miscellaneous articles. There were false positives in the tests, but the number decreased throughout the project. We anticipate that trend will continue in the next phase.

Tests were run at a corrections facility near Luna with prison guards given the device to use on the Luna staff. Plastic knives, guns, and other contraband were hidden on the suspect body and detected with the system. The metal and acoustic detectors were able to see both guns and metal devices. Plastic devices were seen by the acoustic device alone. The guards were very positive about using the device, found it easy to scan, and were not troubled by the false calls since they just patted-down the person in any such area.

In the next phase of this work, Luna will reduce the complexity, size and weight of the system and eliminate the umbilical cable. Input from NIJ recommended contacts will be collected, bringing the existing hardware to appropriate facilities for demonstrations and opportunities for feedback. False calls will be reduced and the alarm system will be modified to incorporate input from the guards and the NIJ reviewers. The form factor of the device will be modified and will incorporate suggestions made by NIJ. Applications beyond correctional facilities will be explored and added to the expanded mission capability.

Commercial partnering will form an important element of the next phase to ensure the device moves from a lab prototype to a practical, cost effective commercial product.

To a great extent, all of the task requirements of this grant were accomplished including the integration of a metal detector with the acoustic device and it's testing in a relevant environment. The detailed results by task follow.

II. Technical Summary

Results and Findings:

Luna Innovations Incorporated has completed its study for the development of an integrated weapons and non-permitted devices prototype (WANDD). As identified in the proposal, the work was broken into 8 tasks. The ultimate goal of this work direction is to produce a practical (low cost, small, hand-held, easily interpreted) device that combines a state-of-the-art metal detector with a new nonlinear acoustic detector that can see and classify both metal and plastic hidden external objects on a human body.

To a great extent, all of the task requirements were accomplished including the integration of a metal detector with the acoustic device. The detailed results by task follow.

Task 1. Requirements Survey

The very first task in this project is to conduct a thorough requirements survey that will help Luna formulate the experiments and tasks that follow this task. To achieve this, we will contact NIJ, NTPAC and other potential users and gather information on the operational needs of the WANDD*. This task will begin in the first month of the project and continue for a full month. Thereafter, periodic discussions will continue till the end of the project.*

Luna contacted numerous members of the Northeast Technology and product Assessment Committee (NTPAC) thru a presentation at their meeting and thru conversations with Alex Fox, Chairman and other participants met at that and other meetings. In addition, Luna spent several days interviewing correction facility workers at a local site on the Virginia Peninsula. In these discussions we identified several key target goals for the intended device. Of particular interest, we focused on the following items:

1) Detection of Plexiglas objects and other non-metallic objects including credit cards, paper money, contraband in plastic bags, contraband in plastic straws, contraband hidden between slit paper cards as examples
2) Detection of hand-made improvised weapons from miscellaneous materials including pen bodies, pikes, springs, kitchen items, CD disk parts
3) Detection of cell phones and any conventional weapon, although conventional weapons are well screened with current practices
4) Use of the device combined with a pat-down to examine and re-examine different body areas as clothing is stretched and moved around
5) Scanner should be light weight, physically small, easy to interpret and be robust

Task 2. Design and build hand-held *acoustic portion of WANDD*

In this task, we will focus on evaluating the various design configurations for building the Wand. Based on the requirements gathered in task 1, the design considerations will include transducer geometry, non-linear acoustic interaction method, propagation distance, alarm indicators, portability and adaptability with the Adam's probe. This task will start in the second month of the project and last for a total period of three months.

A first proof-of-concept device was designed and built for testing using a brassboard (actually wooden board) template and a commercial Adams Electronics ER3000 metal detector. The design used ten 40kHz ultrasonic transducers and specialty electronics we designed to drive the devices and to efficiently couple the electrical energy to generate the nonlinear high-amplitude ultrasonic wave. We tested the individual devices as to power levels (up to 122 dB), ability to generate a parametric beam, and the beam characteristics such as directivity and nonlinear efficiency. The array was mounted in one of Luna's scanners to scan the beam profiles at different distances and frequencies. Initial measurements with the 40kHz array device were encouraging but the propagation distance to get the needed parametric beam was too long. The fabricated array demonstrated impressive sound pressure levels of 142 dB at the 7" focal spot for the ultrasonic beam and 86dB for the parametric acoustic beam. The high Q of the individual transducers led to a narrow frequency band of operation of 2 kHz.

Task 3. Design Optimization and Weapons detection

Based on the input gathered in task 2, we will optimize the design of the 'WANDD' for use in the correctional facilities. The finalized design will be shared with NIJ and NTPAC for feedback and refinement. Laboratory experiments will be conducted at this stage to evaluate the design and test the family of objects supplied by corrections facilities. This task will begin in month 5 and continue till month 7.

We optimized the electrical drive for the 40kHz array and increased the sound pressure levels significantly to 151 dB and 126dB for ultrasonic and acoustic beam measurements respectively. However the 2kHz bandwidth was limiting and we decided to switch to a higher frequency transducer, requiring a complete re-design of the electronics. The re-design uses nineteen ~220kHz transducers in a hexagonal array and has a bandwidth of about 25kHz. Of interest is that the ultrasonic sound pressure levels are above ~95dB over that band and that the nonlinear acoustic sound pressure is between 86dB-96dB over 19kHz of the bandwidth.

Task 4. Integrate Luna's acoustic unit with Adams' metal detector

Luna will coordinate with Adams Electronics for combining the functionality of their existing detector with Luna's non-linear acoustic unit to meet the operational requirements of NIJ. The integration of the technologies will progress through two different stages starting with the mechanical/electrical followed by the signal analysis integration. This task we believe will be one of the key goals for the project. Task 4 will start in month 6 (in parallel with task 3) and continue up to month 11.

The first device was built with the acoustic transducers around the Adams detector package. The two devices exhibited some crosstalk in this configuration, even though we initially tested them out on a pc board. Taking this fact into consideration, we altered the design so that the two devices are at opposite ends of the WANDD holder.

Task 5. Build Prototype and develop test matrix

In this task, Luna will build a lab prototype of the dual-technology instrument that can detect both metallic and non-metallic weapons. The goal of this task is to show that the integrated system can provide an enhanced capability of weapons detection. This task will begin in month 10 and continue for a period of 4 months.

Based on our findings of task 2 and 3, we built a physical prototype of the acoustic system for testing in a matrix of items. We decided to integrate the Adams device so that the two devices are looking at the same area on a body. To accomplish this, the two devices are physically located at opposite ends of the WANDD.

Task 6. Test Prototype

Articles supplied by NIJ will be tested and demonstrated. User feedback will be incorporated to refine the system. Instrument compatibility and detection probability will be studied and appropriate improvements will be made before the prototype can be delivered to NIJ. Task 6 will begin during 14 and last till the end of month 16.

We tested the prototype on a variety of objects including cell phones, guns, improvised weapons such as pikes and plastic knives. The initial tests were run using a tissue simulate (ballistic jell), fabric to simulate clothing and the family of weapons. Using these test conditions, we developed analysis software to fine-tune the operation of the acoustic system. In general, each test used a tone burst of ultrasonics with one frequency fixed and the other concurrent burst as a chirp sweeping between ~ 205kHz to 215kHz. This produces a parametric acoustic beam of ~1kHz-11kHz. The acoustic beam is spatially confined to the ultrasonic beam and therefore produces a refined scan over a focal spot on the body. The WANDD itself is slowly scanned over the area of interest with two lights on the scan handle lighting whenever a reportable event is seen by the metal and/or the acoustic detector.

The signals received by the WANDD are acoustic in nature and are influenced by the objects in the beam. A tube, for example, will have innate acoustic responses when excited over a broad range of frequencies. A gun, therefore, will display different spectral properties than one would see for a button, or a fold of cloth.

The WANDD receives the acoustic data from a microphone and filters out sound that does not fall into the bandwidth of the driver system. The resulting signal is analyzed in the time domain showing the evolution of the acoustics from the initial received chirp to the last sound that fits within the desired time window appropriate for the scan geometry. In addition, the system performs a Fourier transform of the time signals to extract the frequency spectra of the sound. The Luna system uses the time frequency cross plot to evaluate the data and develop time-frequency windows of interest. Such windows are then targeted to extract events that fall within such windows as indicators of hidden objects of interest.

For the operator, the decision making is all transparent driven by the computer. If there is an object of concern, a red or yellow light will come on. This simple approach can be modified so that a hidden object can alert the operator with a sound in addition to the light, perhaps using an earphone on one ear so the person being scanned is not aware of the occurrence.

Luna ran blind tests in our lab for static set-ups. The blind lab tests for the plastic knife were very impressive with detection above 97% and false calls at or below 20%. A cell phone was also scanned and easily detected but in the blind test it was missed. As we looked into this fault it was discovered that the acoustic beam did not insonify the cell location – an error in scanning but not in detection.

NIJ agreed to our doing a demo at a local site in Virginia near our facility instead of delivering the device for testing at their facility. The device was set up at the Virginia Peninsula Regional Jail (VPRJ) for initial testing and for discussions with the corrections experts at their facility. During the first tests, we were pleased to hear the very positive feedback from the corrections people at VPRJ who used the device on hidden weapons placed under clothing worn by the Luna staff at their facility.

Of particular note we were happy that the false positives were not looked upon as problems. With such a finding, the corrections guards just patted down the area, pulled the person's clothing and then scanned on to a new area. Watching them use the device gave us confidence that we had created a device of real value to the customer.

Luna invited senior people from NIJ to attend a demonstration of the device at a second meeting at VPRJ held on March 28, 2008. In attendance at the demonstration was Dr. Frances Scott (Sensors and Surveillance Portfolio Manager, National Institute of Justice), Jack Harne (NIJ Corrections Program Manager) and Jerry Cook (NIJ Center of Excellence). People from Luna at the demo included Dr. Paul Panetta, Dr. Mike Pedrick and Dr. Joseph Heyman.

For the demo a plastic knife was placed under clothing at various locations on Dr. Panetta's body. Dr. Pedrick gave the NIJ folks a quick lesson on how to use the device and turned the system over to the NIJ folks. In a very short time, the NIJ people were comfortable scanning with the device and were able to find hidden plastic objects hidden on Dr. Panetta. There were false positives but again with a pat-down they were passed over.

The NIJ folks hope to use the device at some future sites and develop feedback for Luna as to the efficacy of the prototype to help in shaping a future award to move the prototype to a level able to attract funding for commercialization.

Task 7. Deliver prototype to NIJ and provide technical support

In this task, Luna will deliver to NIJ the prototype that was tested in the lab. Luna will offer technical assistance for operation by NIJ officials. Simultaneously, we will write a design document with estimates of costs involved in supplying various corrections users with the WANDD. This task will take place in month 17 and 18 of the project.

At this time, Luna is holding the system with the plan to use its hardware for a follow-on funded project from the NIJ. Luna hopes to secure additional funding to raise the technology readiness level of the prototype to a point that will attract commercialization support through a partnership with Luna.

Task 8. Commercialization Planning

Luna will contact various corrections facilities in the US to brief them on the capabilities of the WANDD. We will prepare a business plan to commercialize the instrument. Working with Adams Electronics, we will identify various security related applications as well as competitors for the WANDD and begin the commercialization process. This task will take place in parallel with task 7 during the final two months of the project. We will involve various Luna senior management personnel as necessary.

Luna has talked to a number of major national security companies who have expressed interest in this technology. To move to the next level of interest, the TRL of the prototype should be carried to the next level. It is our estimate that we are now at TRL 5. A Phase II from NIJ, perhaps in partnership with a second government office, will enable Luna to invest more development into the analysis software and fine-tuning the hardware bringing the device to a sufficient development level for commercialization.

During the NIJ meeting in Orlando October 24,25, 2007, an interesting discussion arose concerning the market realism of the various developers who were funded by NIJ. Luna had explored that realism earlier in discussions with the Northeast Technology Product Assessment Committee (NTPAC) in their meeting of June 29,30, 2005. Those conversations and subsequent discussions with members of the corrections community helped the Luna project focus on an ultimate cost boundary in the several thousands of dollars, in some volume production.

Therefore it was no surprise that the Luna approach was identified at the Orlando meeting as one of the only talks that addressed the needs of the community as to projected cost targets. Since winning the NIJ Phase I, we have continued to focus on a development that is targeting that price range. The next Phase II funding will permit the technology development and software advancement to reach the technical and design considerations that are needed to move this device to attract funding to commercialize this device.

Conclusions:

Luna has demonstrated that the use of nonlinear acoustics brings enhanced detection for weapons and especially non-metallic devices of concern such as plastic weapons. A very significant development has been demonstrated bringing two measurement modalities into a single scan. One such modality did not exist before this funded project from NIJ. This new capability opens the door for hand-scanning for hidden plastic and other non metallic objects carried by a person in a corrections environment. This device can be used for both incarcerated people and for their visitors, although in different modes of use.

The ultimate system based on these findings has the potential to be cost effective. As part of the future work we will focus on bringing the production for volume levels to 1-3K. The integration and testing went smoothly and the ROC was defined based on initial (or limited) testing. Improvements in the analysis algorithms and software will speed the technique up and improve its rate of false calls.

Implications for criminal justice operations:

Based on feedback Luna received by corrections professionals, we are optimistic that this device has very significant value for corrections operations. In their hands, the corrections people voiced their pleasure with the ability of the device to find plastic items hidden under clothing. They learned how to use the device very quickly and were finding objects that we had not even considered such as gum and chapstick tubes under socks.

Although there is further development required for this technology, it is clear that it can play a significant role in enhancing the safety at corrections facilities and thoroughness of examinations. By keeping the final cost of a volume device as the key parallel driver along with detection of non-metallics, the WANDD project was very successful and is ready for the next phase of support.

The proof of concept hardware and initial algorithm has shown high detection efficiency for plastic and metal weapons hidden under clothing, outside a person's body. Future work should focus on three key areas: 1) improving the detection efficiency, 2) decreasing false positives, and 3) increasing the scanning speed. The work from this project has identified specific hardware and software activities to reduce false calls and improve detection efficiency including refining the decision software, reducing the acoustic beam width, increasing the power, and compensating for the variable curvature of human bodies with hardware and software advancements. An increase in the scanning speed can be achieved by increasing the repetition rate by optimizing the electronics and transducer selection. In the future phases we will work to balance the sophistication of the instrument and power requirements with the need to provide a commercial instrument that is a light, portable, battery operated, handheld, and cost competitive. An important part of next phase of this work will be to get feedback on the functionality and improvements needed through demonstrations and feedback from the correction community. Obtaining this feedback early in the next phase will be important for prioritizing the hardware and software advancements and targeting the appropriate development path.

III. Detailed Task Review

The following sections detail progress in the context of the tasks identified in the original proposal. The information presented in this section contains both a compilation of reporting to date along with additions from the current period of effort (shown below in Table I).

Table I: Schedule highlighting the current period of effort

Task \ Month	1	2	3	4	5	6	7	8	9	10	11	12	13	14	15
1: Requirements Survey															
2: Design/Build handheld portion of acoustic WANDD															
3: Design Optimization and Weapons Detection															
4: Integration of Luna's acoustic unit with Adams metal detector															
5: Build prototype and test matrix															
6: Test prototype															
7: Deliver prototype to NIJ and provide technical support															
8: Commercialization planning															

a. Task 1: Requirements Survey

The requirements survey was moved from month 1 of the program to months 4 and 5 in order to include more comprehensive questions based on the results of some initial testing. Luna's Questionnaire on Contraband Detection was submitted to Alex Fox on July 3, 2007 (see Appendix A). This questionnaire was then posted on the NTPAC website and responses are currently being collected. A response was requested for July 26th. An initial response was received from Donna Collins, Deputy Warden for the Rhode Island Department of Corrections. Some highlights of this response are shown below.

> *"We currently have 6 hand scanners in use and more available for hospital/trip bags. On average, we may replace one per year."*
>
> *"Primary objective is to identify and locate weapons…regardless of the material they are made of. Detection of Plexiglas and non-metal weapons is currently difficult. Eyeglass stays and other objects that are made of alloys pose a challenge. Currency – paper and coin – is a problem. Cell phones and electronic devices are a potential threat. Current facility is a very secure building with primarily non-contact visits. Rate of contraband findings does not reflect level of concern for the same. Frequent strip searches and a highly sensitive walk through metal detector keep contraband findings at a minimum. Population is 100."*
>
> *"Typically, contraband is secreted in a body cavity. Have had recent incidents of contraband hidden in hair (dread locks)."*

It was later determined that official survey responses from NTPAC members could not be obtained. Survey inputs were then sought via telephone and face to face interviews. Feedback from VPRJ Superintendent John Kuplinski and Rhode Island DOC representative Jim Bailey added valuable insight to this effort. This resulted in the inclusion of additional concealed items in the test matrix such as drugs, currency, and credit cards. The suite of concealed objects considered for this testing was updated based on inputs from corrections officials discussed under task 1. Major weapons of concern are often those fabricated within the facility confines. Technologies which could ultimately introduce the capability for noninvasive inspection of body cavities would be very advantageous to the security of a corrections facility. The current list of concealed objects under test include: plastic knife, gun, cell phone, paper currency, credit card, drug simulants, and a pen-pike.

b. Task 2: Design and Build Handheld WANDD

As part of the development of the WANDD prototype, we first acquired a sample of the Adams Electronics ER3000 metal detector, which is shown below in figure 1. To incorporate both designs into the prototype, we had to modify the circuitry of the EL3000 to produce a digital output signal which would indicate detection by the Adams metal detector. Based on discussions with Adams electronics, we were able to modify the buzzer circuit to produce such a signal. By having the EL3000 early in the testing and development process we were able to design the prototype board to have the ultrasonic transducers in a ring around the detection circuit of the metal detector. This allows us to test for cross-talk interference between the metal detector and the ultrasonic driver electronics at the most sensitive point of the Adams detector.

Figure 1: Adams Electronics ER3000 metal detector.

For the first set of transducers to test, we selected 40 kHz air coupled transducers from American Peizo Technologies, model 40T-16. These are highly efficient transducers with a output sound pressure level in excess of 120dB with a maximum 45 V peak to peak drive signal. The response of the transmitter version of the transducers is shown below in Figure 2 and the resulting electrical impedance curves are shown in Figure 3. To develop the driver electronics to generate the ultrasonic frequencies and the nonlinear difference frequency, we built the first prototype board shown below in schematic form in Figure 2 and as a completed board in Figure 3. This design was based on the concept drawing of figure 6 in the proposal.

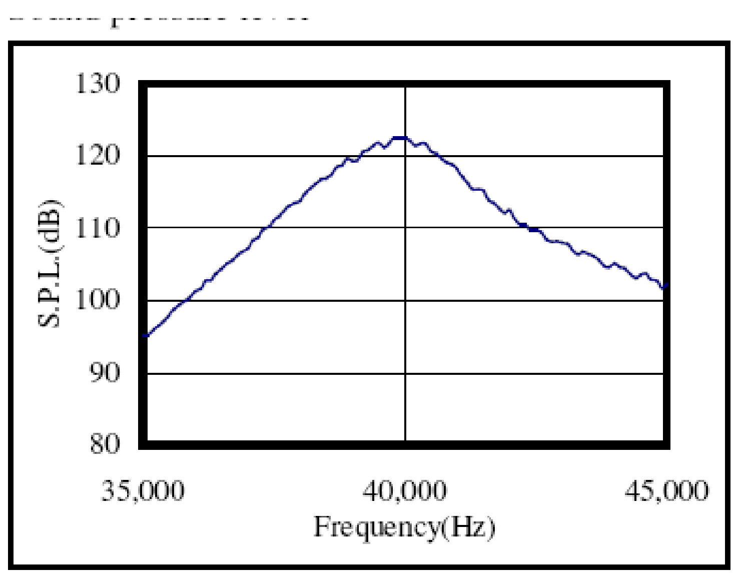

Figure 2: Transmitter characteristics for the APT 40T-16 transducers

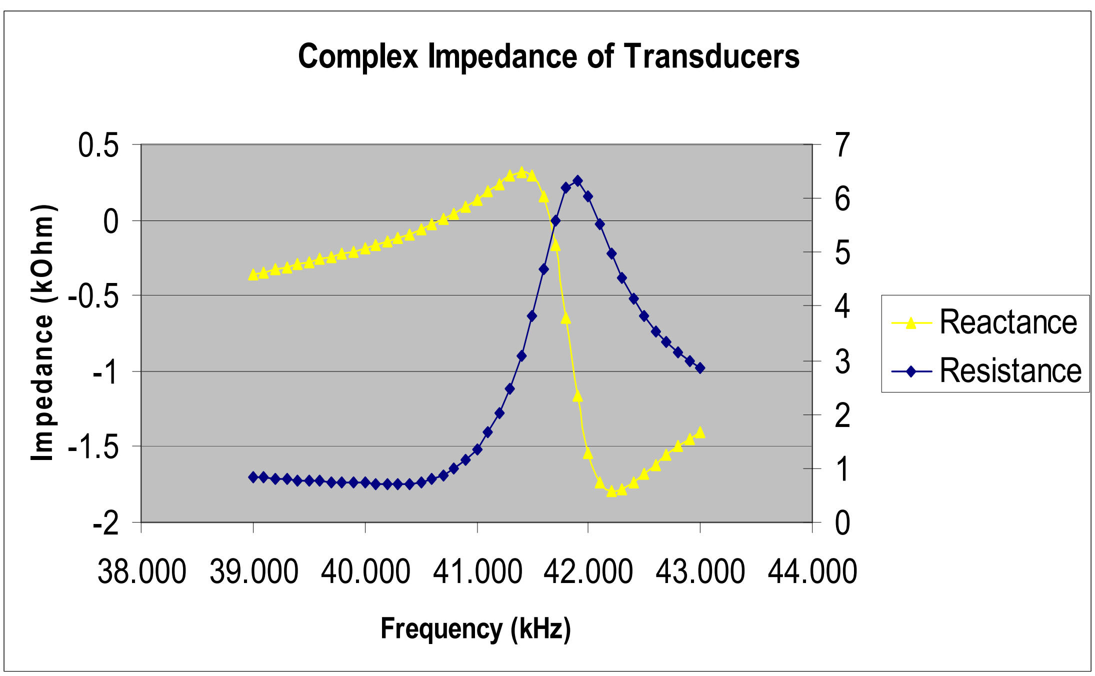

Figure 3: Electrical response characteristics of the APT 40T-16 transducers.

These transducers were selected for their low cost (less than $7 in quantity) and for the high transducer efficiency. One restriction of the transducers is the narrow bandwidth. As part of the project, we have investigated using electrical matching networks to broaden the bandwidth of the transducers to permit a larger chirp signal to be generated by the nonlinear effect. An example of the matching networks is shown below in Figure 4.

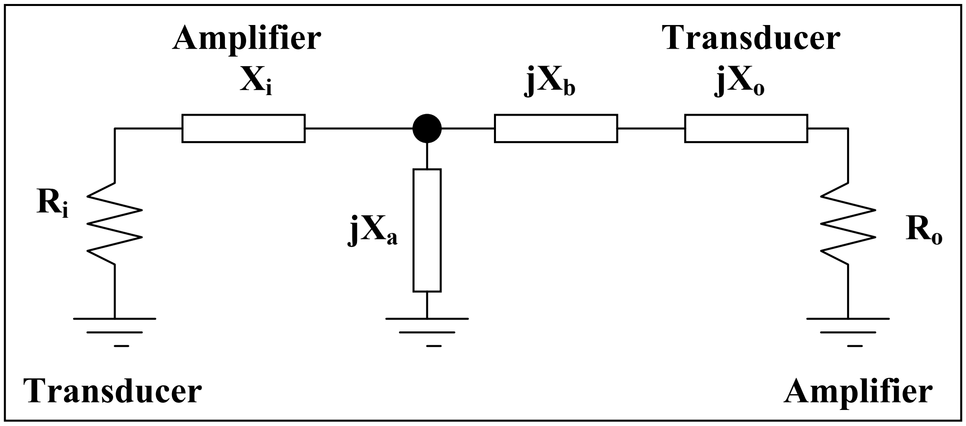

Figure 4: An example of a matching network for the 40T-16 APT transducers in either a voltage step-up mode with a high Q of approximately 20 or a lower Q of 0.4 to broaden the bandwidth of the transducers. This matching network assumes that the network items are purely reactive components.

The basic block diagram for the transmitter and receiver electronics is shown below in Figure 5. We are generating the difference frequency (f1-f2) by controlling the frequency and amplitude of two Agilent function generators operating in burst mode, with a common 10 MHz clock to reduce phase jitter. The burst outputs of each function generator is then summed together and then sent to the custom amplifier shown below in Figure 6. The B&K microphone was used to detect both the ultrasonic signals (typically 39 and 41 kHz) and the difference frequency (2 kHz). We added a Krone-Hite adjustable audio filter and amplifier to amplify the difference frequency and provide additional rejection of the ultrasonic frequencies. Additional filtering using a digitally implemented FIR low pass filter was done in the LabView analysis program. The output of the filter was acquired for analysis using a 20 MHz data acquisition card and a laptop computer. Typically most of the data was acquired using a data acquisition rate of 600 kHz.

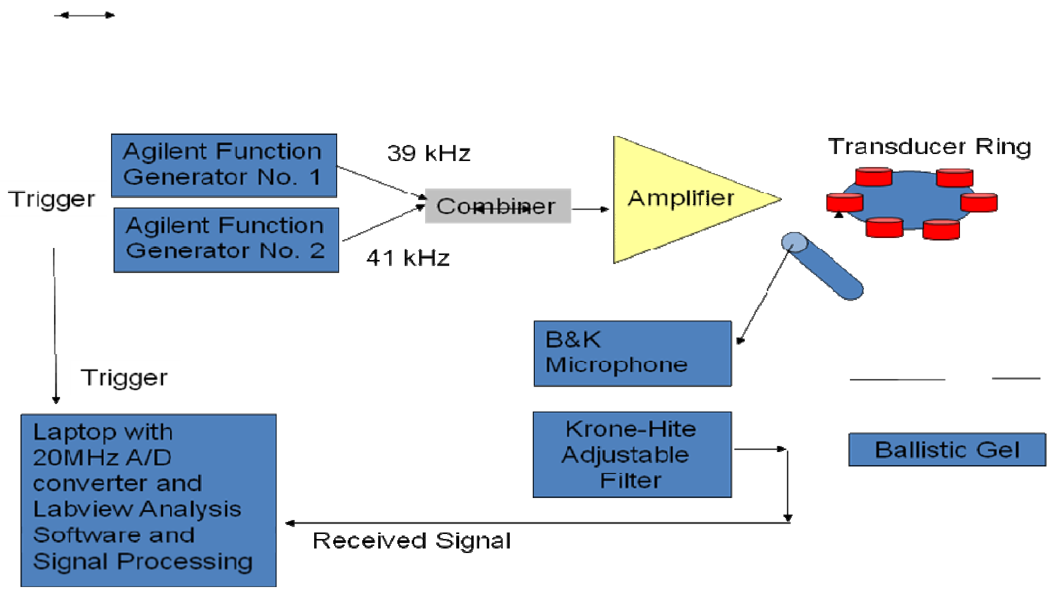

Figure 5: Block diagram of the electronics for the transducer ring and preliminary tests.

To maintain maximum flexibility in the initial testing and to permit the evaluation of different transducers we selected to build the amplifier in multiple gain stages to maintain a high bandwidth and slew rate. The first design characteristic was the choice of the primary high voltage amplifier, with the choice of the PA09 amplifier from Apex Microtechnologies. This PA09 amplifier has a relatively high gain bandwidth product of 150 MHz or 1.5 MHz with a gain of 10. It also has a high slew rate and can produce outputs up to 150V peak to peak and up to 5A of current. This amplifier has a large heat sink and an associated fan which can be seen in the completed board assembly.

The first stage was a buffer circuit matched to the 50 Ohm impedance of the input BNC cables. The second stage was the low level gain stage and the final gain stage was using a high power Apex amplifier. We selected Analog Devices AD811 video amplifiers for use in these gain stages. The gain in the second stage was adjustable.

To maintain signal fidelity, series resistors were used to limit the current into the transducers and to limit cross talk between the individual transducers. These are shown in Figure 6 between the test point of 45V and the transducers. As part of the testing process, we had to modify these matching resistors and to increase the gain of the amplifier.

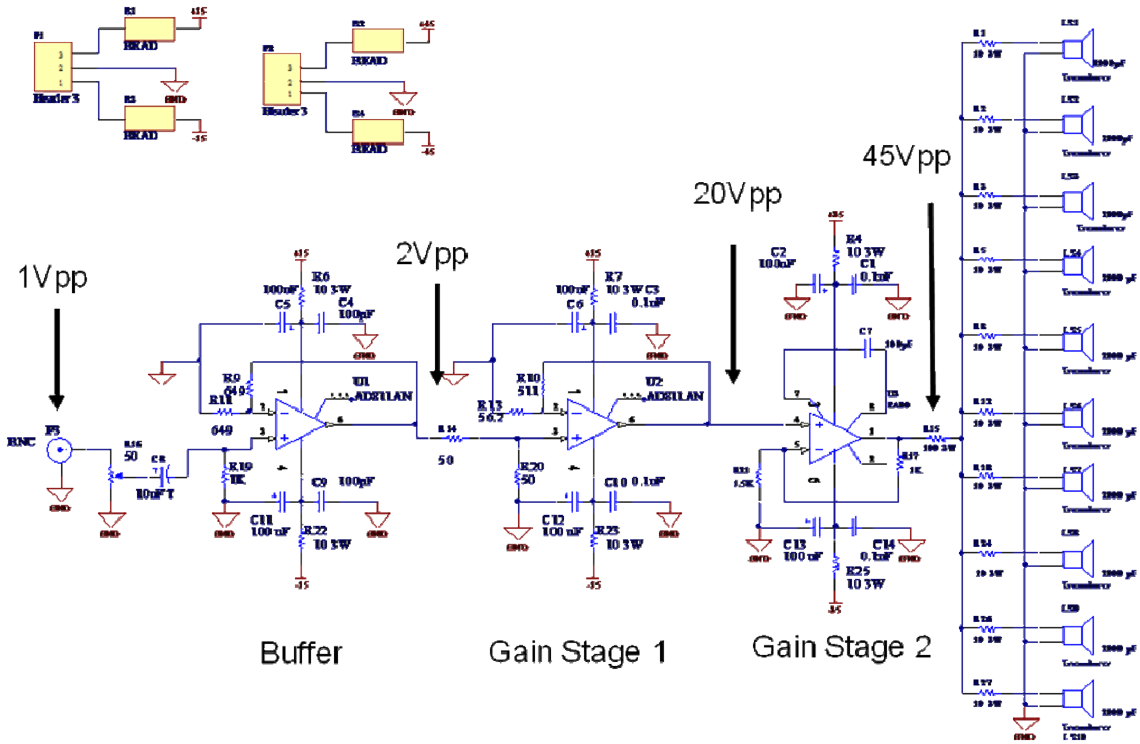

Figure 6: Custom Amplifier to drive the transducers shown on the right hand side of the schematic. The first stage was a buffer circuit matched to the 50 Ohm impedance of the input BNC cables. The second stage was the low level gain stage and the final gain stage was using a high power Apex amplifier.

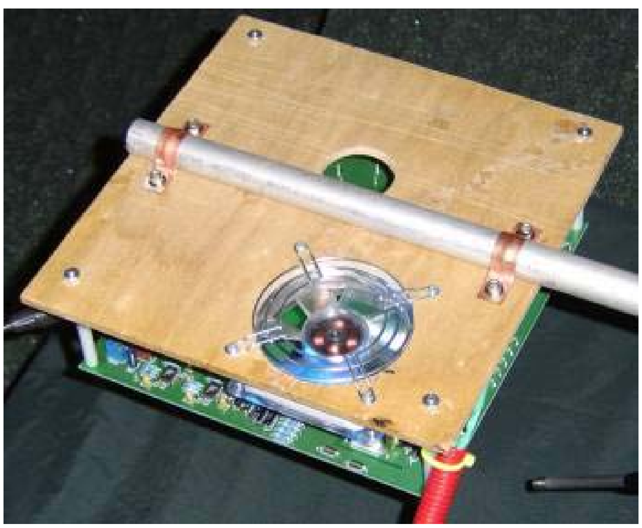

Figure 7: Complete custom amplifier board in the process of testing.

c. Task 3: Design Optimization and Weapons Detection

Initial testing of the laboratory unit consisted of characterizing the ultrasonic and non-linear acoustic beam profiles. This was achieved through a series of automated scans using Luna's large volume C-Scan system. The transmitter was mounted in the tank and the receiver was raster-scanned at various distances from the transmitter resulting in several beam cross sections. Photographs of this test are shown in figure 8 and the results in figure 9. Each cross-sectional image consists of a 180 x180 mm scan area with a 2 mm step size. A slight mechanical focus was applied to the transducers by manually tilting each element in toward the center of the annular array. Note the focal length is approximately 7". The ultrasonic sound pressure at the focal spot is 142 dB-SPL.

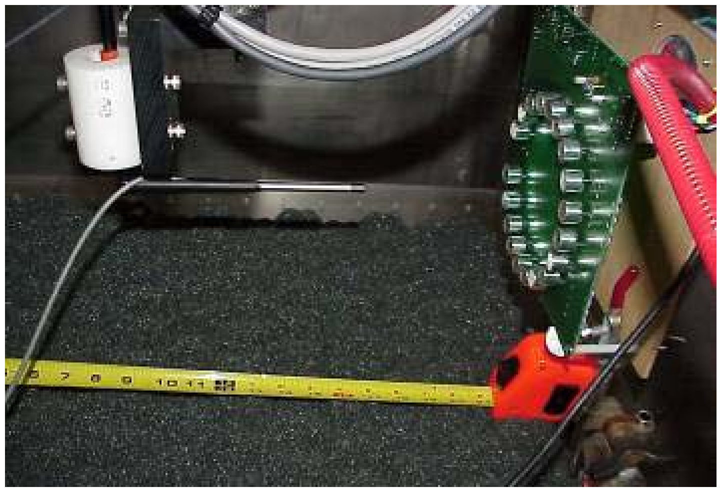

(a)

(b)

(c)

Figure 8: Photographs of the scanning setup used to generate the results shown in figures 8 and 9 for the vertical and lateral beam cross sections.

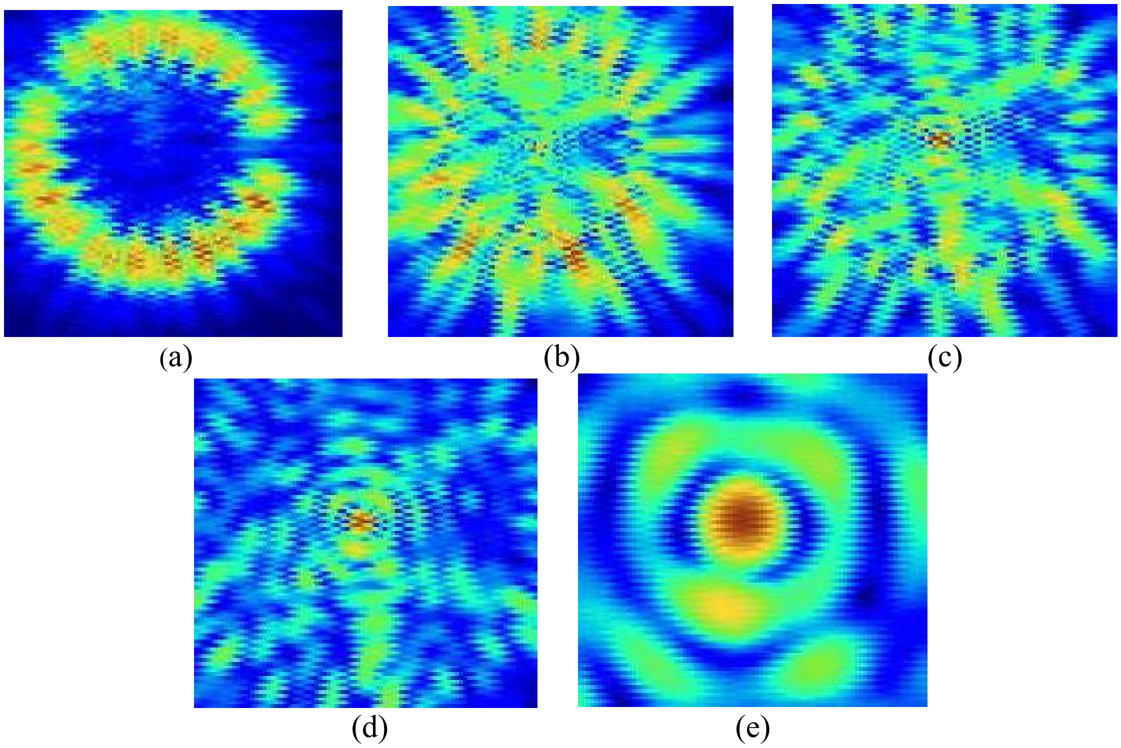

Figure 9: Vertical beam cross sections for a 40 kHz, 16 cycle toneburst excitation taken at (a) 1 inch, (b) 3 inch, (c) 5 inch, (d) 7 inch, (e) and 24 inches from the transmitter.

Lateral cross-sectional scans were then taken both at 40 kHz and at a difference frequency of 2 kHz achieved by mixing two tonebursts at 39 and 41 kHz. Note the reduction in side lobes for the non-linear acoustic beam compared with the ultrasonic beam. The sound pressure levels at the focal points were 142 dB-SPL and 86 dB-SPL for the ultrasonic and non-linear acoustic beams, respectively. The scan dimensions are 760 mm x 50 mm. These scans are shown in figure 9. A screenshot from the developed software showing the mixing of two ultrasonic frequencies is shown in figure 10.

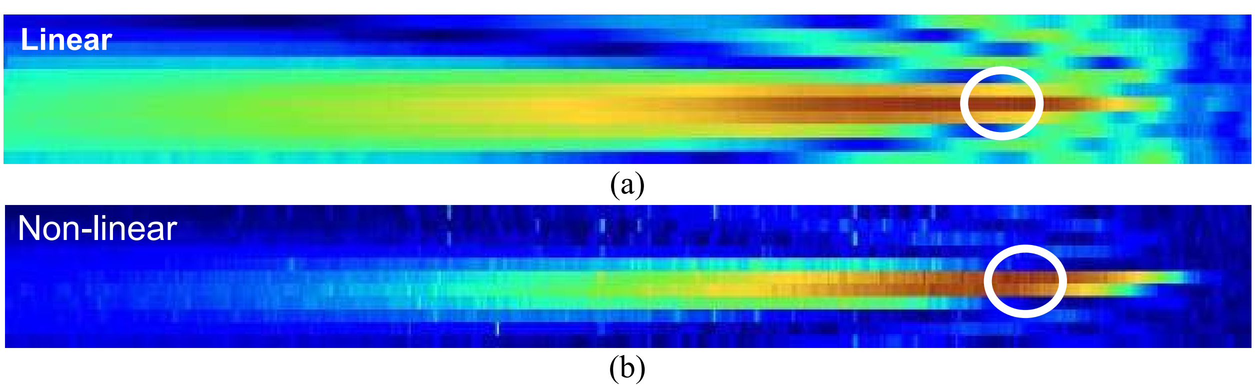

Figure 10: Lateral beam cross sections for (a) 40 kHz ultrasonic beam and (b) 2 kHz non-linear acoustic beam achieved by mixing two ultrasonic tonebursts at 39

and 41 kHz. The sound pressure levels for the ultrasonic and non-linear acoustic beams were 142 dB-SPL and 86 dB-SPL, respectively.

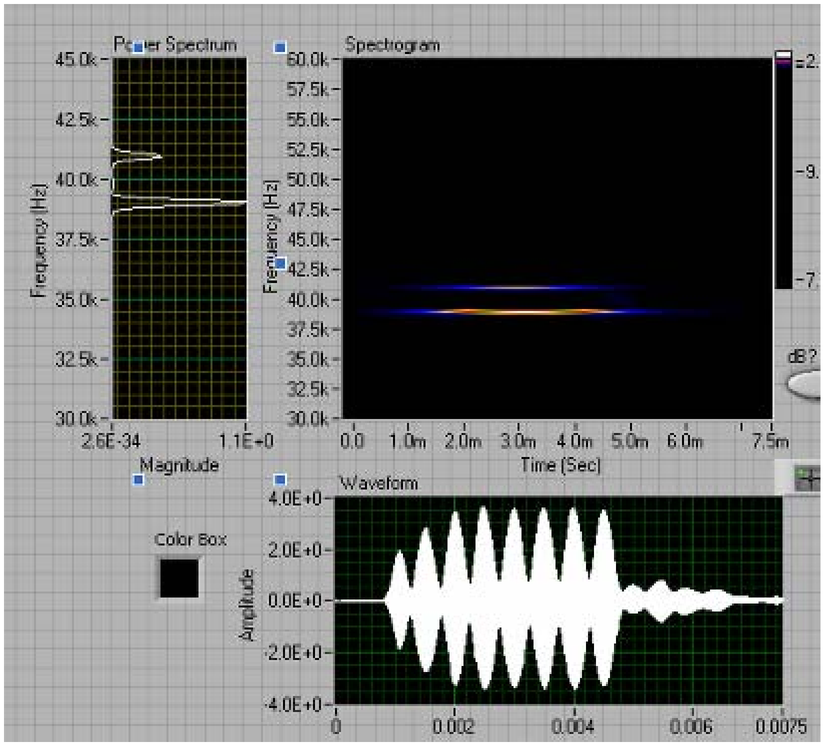

Figure 11: Screenshot from the software routine developed for system control and signal processing showing the mixing of two signals at 41 kHz and 39 kHz.

Tests were conducted to analyze the unit's capability to penetrate fabric and maintain adequate sound pressure levels. A photograph of this setup is shown in figure 12. The receiver was positioned at approximately the focal spot of the transmitter array. Sound pressures were measured at the receiver for two scenarios, one where fabric was placed in the sound path and one without fabric for comparison. These tests were repeated for a 40 kHz ultrasonic toneburst and a non-linear acoustic toneburst at 2 kHz. The test showed that the sound pressure level for the non-linear acoustic signal where inadequate. The electronics were modified to increase the voltage at the transducer from approximately 17 V_{pp} to approximately 40 V_{pp}. This was done as previously mentioned by increasing the overall gain of the two final gain stages by a factor of 2, increasing the power supply voltages and by reducing the current limiting resistor R95 from 100 Ohms to 10 Ohms. This increased the drive signal on the individual transducers from approximately 12V to 40V. As a result of this, we were able to reduce the gain in the Krone-Hite filter/amplifier and increase the signal to noise ratio. The aforementioned tests were repeated. A summary of those results are shown in Table III.

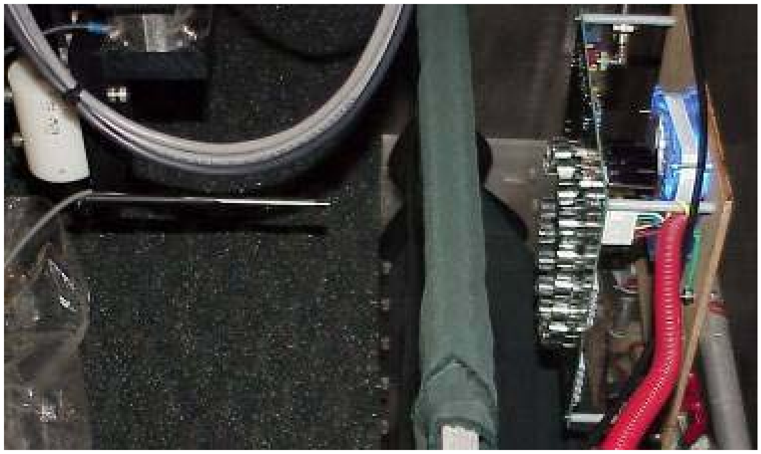

Figure 12: Photograph showing the characterization of sound pressure through a fabric. The receiver is approximately 7" from the transmitter and the fabric (green in the photo) was draped halfway between them.

Table III: Results of sound pressure analysis through fabric for the initial and modified laboratory unit.

Freq	Non-linear	Scenario	Initial Pa	Initial dB-SPL	Modified Pa	Modified dB-SPL
40 kHz	No	No shirt	250	142	720	**151**
40 kHz	No	Shirt	79	132	242	142
2 kHz	Yes	No Shirt	0.4	86	41.6	126
2 kHz	Yes	Shirt	0.08	72	3.3	**104**

Note the modified electronics yielded a significant increase in the sound pressure levels for each of the configurations. It was expected that the decrease of sound pressure through the fabric would be less severe for the non-linear acoustic signal versus that of the ultrasonic one. As evident in Table III, this was not the case. This is most likely due to an inefficient mixing of the two ultrasonic frequencies necessary to generate the non-linear acoustic signal. Achanta, et al[1] have shown that the average force integrated over one cycle can be described by:

$$\left[\rho_0 c \delta_0 A_1^2\right]/2 \qquad (1)$$

[1] Achanta, A., McKenna, M., Guy, S., Malyarenko, E., Lynch, T., Heyman J., Rudd, K., Hinders, M. Nonlinear Acoustic Concealed Weapons Detection. *Materials Evaluation*, Vol. 63 (12), pp. 1195-1202, 2005.

where ρ_0 is the static density of the medium, c is its adiabatic sound velocity, δ_0 is incremental change in density associated with the acoustic wave and A_1 is the oscillatory displacement amplitude in the presence of the acoustic wave. All of these parameters are physical properties associated with the medium excluding A_1. Thus, the average force over one cycle can only be increased by increasing the drive voltage, thereby increasing the displacement associated with the acoustic wave propagation. However, the overall force generated in a fixed path length can be increased by increasing the number of cycles. This can be achieved by increasing the frequency, increasing the overall nonlinear conversion efficiency in the generation of the difference frequency. The efficiency of the nonlinear conversion process also depends on the propagation distance and the attenuation of the ultrasonic signals. By increasing the frequency of the transducers, we can increase the conversion and reduce the distance required for sufficient amplitude of the difference frequency. Therefore, the losses of the ultrasonic signal through the fabric have an additive effect on the losses of the non-linear acoustic signal.

After the initial characterization of the system, its weapons detection capability was analyzed. An experimental setup was used consisting of ballistics gel (as a human tissue stimulant), the fabric, and various contraband materials. Much of the initial testing was done using a standard box cutter. The same scanning system used for generating the beam profiles was modified to accommodate the setup. The laboratory unit was scanned over concealed contraband and the non-linear acoustic signatures were analyzed with algorithms implemented in LabView. Photographs of this experimental setup are shown in figure 13.

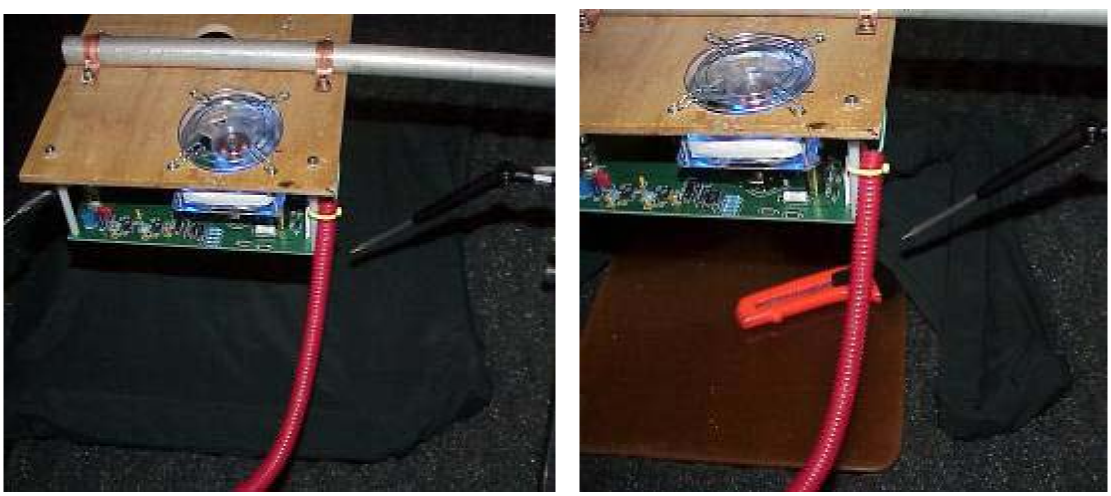

(a) (b)

Figure 13: Photographs of the experimental test used to analyze the laboratory unit's concealed weapons detection capability. The photograph in (b) simply has the fabric pulled back to show the weapon, the actual testing was done under the configuration shown in (a).

Tests were conducted by scanning the system overtop and away from the weapon. To verify the validity of the non-linear acoustic signature generated from overtop of the weapon, the test was repeated with the weapon moved to a different location. The test configurations are shown schematically in figure 14 and the associated non-linear acoustic signatures in figure 15.

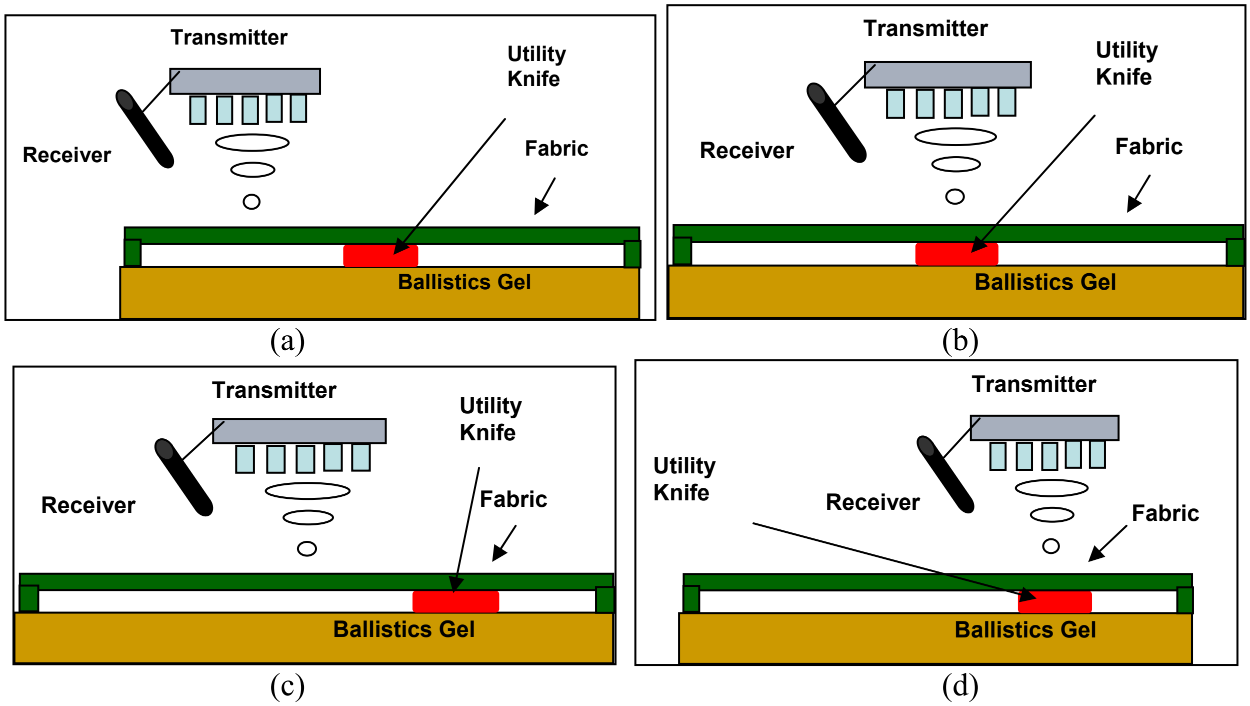

Figure 14: Schematic representation of the testing configurations associated with the results shown in figure 14. These will be identified as (a) configuration 1 (b) configuration 2 (c) configuration 3 (d) and configuration 4.

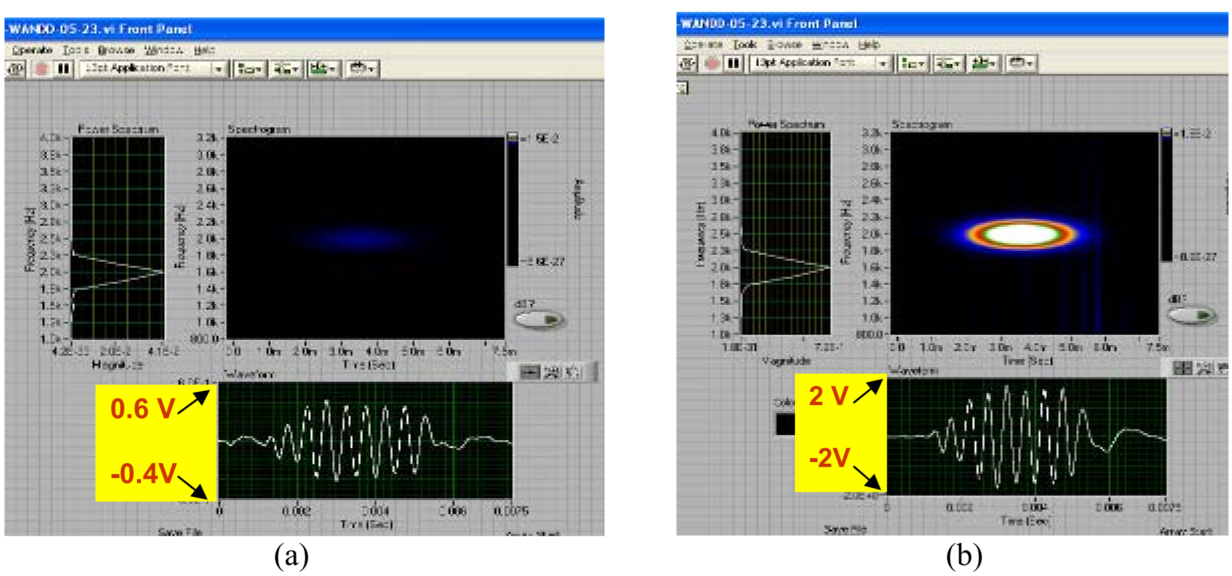

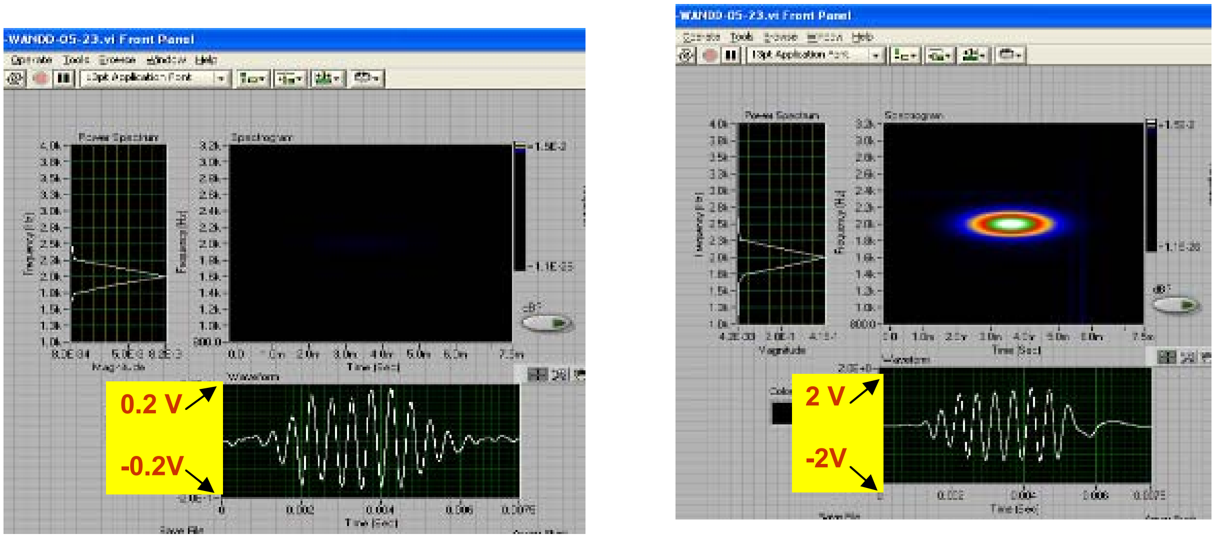

(c) (d)

Figure 15: Non-linear acoustic signatures for (a) configuration 1 (b) configuration 2 (c) configuration 3 (d) and configuration 4 as shown schematically in figure 13.

In this configuration, the system has two major limitations. The first is the narrow-banded nature of the transmitter which severely limits the capability of generating non-linear acoustic signals at frequencies greater than 4 kHz. The second issue is the aforementioned inefficiency in generating the non-linear acoustic signal due to the relationship between the wavelength and the sound path prior to impinging on the fabric. Both issues were mitigated by transitioning to higher frequency, broader band sources. Several sources from Massa Products Corporation were obtained. Transducer at 150 and 210 kHz were procured, the transmitter characteristics of which are shown in figure 16.

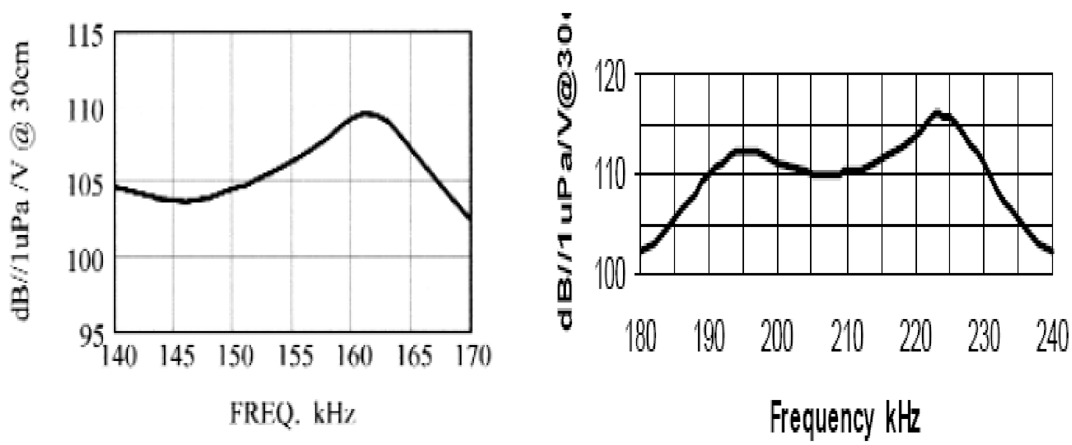

(a) (b)

Figure 16: Transmitter voltage responses for (a) 150 kHz and (b) 210 kHz TR-2400 series air ultrasonic transducers from Massa.

Through-fabric propagation tests were repeated with the new set of transducers in order to confirm the earlier supposition that higher frequency transducers would yield more beam mixing efficiency over a fixed path length. The tests were conducted as previously described and the results are shown in Table IV. Because of the increased bandwidth of these transducers, non-linear acoustic signals were generated ranging from 6 to 12 kHz. This was done to demonstrate the capability of the system to operate with a chirp excitation. This provided a more comprehensive signature and became the foundation for enhancing the systems concealed weapons detection capability.

Table IV: Results of Through-fabric propagation tests conducted with the 210 kHz, broadband transducers

Frequency (kHz)	Nonlinear	Scenario	Sound Pressure (dB-SPL)
210	No	No Shirt	100
210	No	Shirt	86
12	Yes	No Shirt	67.6
12	Yes	Shirt	56.9
11	Yes	No Shirt	70.2
11	Yes	Shirt	58
10	Yes	No Shirt	69
10	Yes	Shirt	58
8	Yes	No Shirt	65.7
8	Yes	Shirt	56.7
6	Yes	No Shirt	63.5
6	Yes	Shirt	53.9

Currently, the electronics are being modified to increase the drive voltage from 40 V_{pp} upwards of 65 V_{pp}. Notice also that the overall sound pressures of Table IV are lower than the earlier sound pressures shown in Table III. Recall that the original configuration contained 19 transmitters whereas the new tests were conducted with only one transmitter. More transmitters were procured from Massa to complete a multi-element array. This will help increase the overall sound pressure emitted from the transmitter. At the research stage, these transducers are cost prohibitive ($200-$400/transducer) however, in manufacturing quantities (i.e. >1000), the unit cost is reduced by a factor of 10. This cost is more acceptable for realizing a unit at the desired price point detailed in the proposal.

Based on the results of the last reporting period concerning beam profiling, a new array geometry was implemented with the higher frequency transducers obtained from Massa. The new array consists of 19 elements in a hexagonal pattern. The goal of this transition was to minimize the "dead zone" in front of the array (which was approximately 5 to 6" for the previous annular version) and to slightly broaden the focal spot of the emitted sound waves, making the system more conducive for scanning. A photograph of this array configuration is shown in Figure 17.

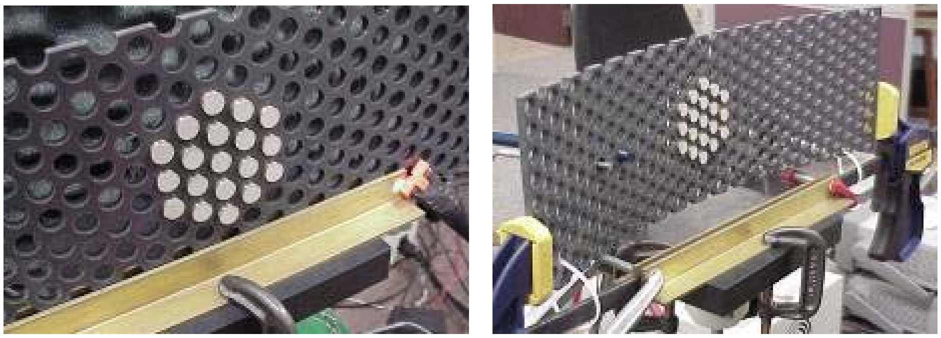

Figure 17: Photographs of the new 19 element hexagonal array. The mesh holder was machined to fit each element giving the added capability of changing the array configuration as well as generating a cylindrical focus as shown in the left photograph.

One benefit of the transition to higher frequency transmitters was increased nonlinear coupling efficiency. This concept was demonstrated with a single element in the previous report but was further tested with the hexagonal array to assess its capability to produce sufficient acoustic power levels. The test was also used to determine the usable frequency range of the broader band transducers. This information was then applied to define the frequency limits of the chirp excitation function described later in this section. Table V shows the results for sound pressure levels of both the linear ultrasonic and non-linear acoustic signals over a range of frequencies both with and without fabric in the acoustic path between transmitter and microphone. Note there is a general decrease in the signal loss through the fabric ranging between 1 and 6 dB for the various frequencies.

Table V: Sound pressure levels through fabric at various frequencies

Linear Ultrasonic Signal				Non-Linear Acoustic Signal			
Frequency (kHz)	Sound Pressure Levels (dB)		Signal Loss Through Fabric (dB)	Frequency (kHz)	Sound Pressure Levels (dB)		Signal Loss Through Fabric (dB)
	No Fabric	Fabric			No Fabric	Fabric	
225	105.7	92.9	**-12.8**	5	75.7	63.1	**-12.6**
224	107.8	93.3	**-14.5**	6	76.5	67.1	**-9.4**
223	107.3	93.4	**-13.9**	7	75.9	67.2	**-8.7**
222	105.5	91.9	**-13.6**	8	80.7	68.2	**-12.5**
221	105.7	91	**-14.7**	9	82.1	72.4	**-9.7**
220	107	90.4	**-16.6**	10	84.6	70.1	**-14.5**
219	106	90.8	**-15.2**	11	86.5	74.6	**-11.9**
218	104.3	88.2	**-16.1**	12	85.8	73.1	**-12.7**
217	104.5	91.4	**-13.1**	13	88.2	75.5	**-12.7**
216	104.3	90.7	**-13.6**	14	89.2	74.7	**-14.5**
215	106.6	89.8	**-16.8**	15	88.4	78.1	**-10.3**

Although a significant improvement in nonlinear coupling has been realized, the sound pressure levels at this point were too low for an adequate detection system. In order to increase the sound pressure level, the drive voltage was increased from 30 V to 70 V through the use of a step-up transformer. The peak drive voltage rating for the transducers is 50 V at 10% duty cycle. This drive voltage can be increased by decreasing the duty cycle. In our case, the duty cycle was reduced from 10% to 1% to allow for safe operation at 70 V. The arbitrary waveform amplitude was tailored to eliminate distortion from the amplifier while maintaining this higher drive level. It was discovered the amplifier distortion had been adversely contributing to the nonlinear coupling efficiency even at the 30 V drive level.

Although the nonlinear shock-distorted waveform does not severely affect the sound pressure level at the linear ultrasonic frequency, it has a significant effect on the generation of the beam-mixed acoustic signal. This effect is evident in table VI which shows results from the modified system for sound pressure levels of the ultrasonic and nonlinear acoustic signals with fabric between transmitter and receiver. Comparing these results with those shown in table V one sees approximately a 6 dB average increase in sound pressure at the ultrasonic frequencies but a 20 dB average increase in sound pressure at the nonlinear acoustic frequencies.

Table VI: Sound Pressure levels through fabric at various frequencies for modified system

Linear Ultrasonic Signal				Nonlinear Acoustic Signal			
Frequency (kHz)	Sound Pressure Level (dB)	Frequency (kHz)	Sound Pressure Level (dB)	Frequency (kHz)	Sound Pressure Level (dB)	Frequency (kHz)	Sound Pressure Level (dB)
200	94.6	213	94.4	5	83.1	18	92.2
201	96.6	214	98.9	6	86.0	19	93.7
202	93.8	215	96.5	7	85.7	20	97.2
203	95.9	216	96.2	8	84.1	21	96.46
204	96.18	217	97.2	9	85.0	22	97.5
205	96.1	218	97.1	10	88.6	23	96.9
206	95.3	219	96.9	11	90.5	24	94.7
207	96.1	220	99.7	12	89.6	25	95.9
208	97.1	221	98.8	13	90.0		
209	97.2	222	98.1	14	91.1		
210	97.8	223	97.9	15	92.2		
211	97.9	224	100.5	16	94.8		
212	97.5	225	97.8	17	94.3		

These tests were also useful in defining the appropriate frequency ranges for the chirp signal. Results shown in tables V and VI were generated with the original setup which consisted of adding two fixed frequency signals from two separate function generators resulting in a single difference frequency signal. A more robust approach would include a band of difference frequencies to help promote sound interaction with a wider variety of materials and geometries. To achieve such a drive signal, an arbitrary waveform was defined which adds a fixed frequency signal with a frequency band chirp. The result is a band of difference frequencies. The chirp based approach is shown in Figure 18.

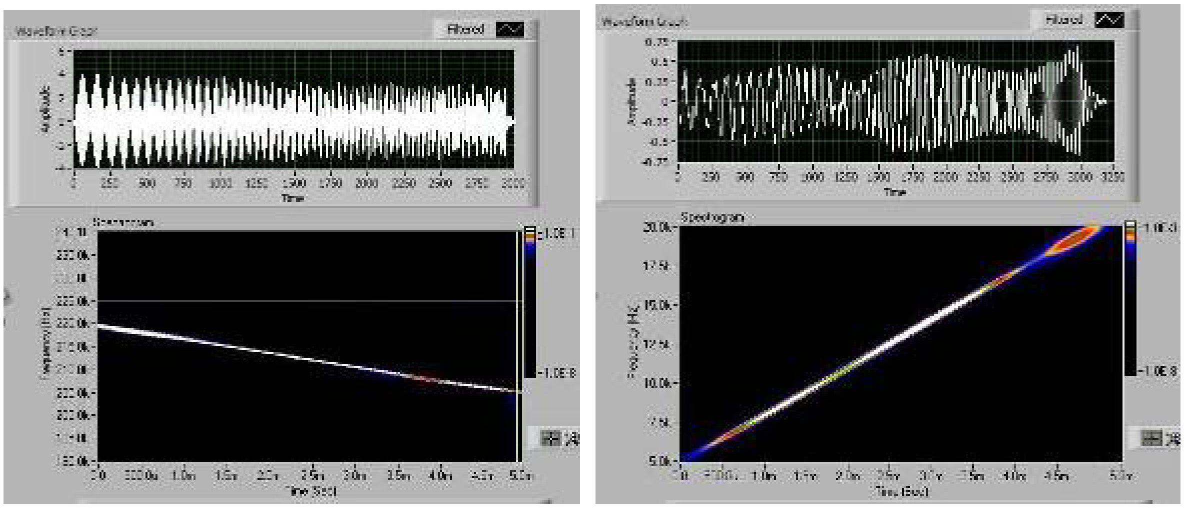

Figure 18: (Left) Excitation signal which includes a constant 225 kHz toneburst added to a chirp beginning at 220 kHz and ending at 205 kHz. (Right) The resulting nonlinear acoustic signal generated by the difference between the 225 kHz signal and the chirp. Notice the difference frequency ranges from 5 kHz to 20 kHz.

Initial weapons testing with the modified system was conducted with the configuration shown in Figure 4. This approach was based on the findings of the previous reporting period that oblique incidence could help to isolate signal contributions from a concealed object from energy scattered or reflected from the fabric. The two goals for testing were to evaluate the sensitivity of the system as well as investigate several signal processing techniques capable of producing signatures for detection. Tests consisted of collecting waveforms both with and without a variety of concealed objects. Signals were analyzed in the time domain, frequency domain, and joint time frequency domains. A survey of these initial results is shown in Figure 19.

Figure 19: Initial test configuration used with modified

Each screenshot shows the three aforementioned signal representations. The top graph shows the time domain signal, the middle graph shows the frequency domain representation, and the bottom graph represents the joint time frequency representation. The left column shows data with no concealed object while the right column represents the data obtained with the identified object present. Differences between the data with and without concealed weapons can be identified in each of the three representations though the joint time frequency representation is most easily seen graphically. The general trend is an increased amplitude response at the higher frequencies (15 to 25 kHz), though it is not readily identifiable for each object.

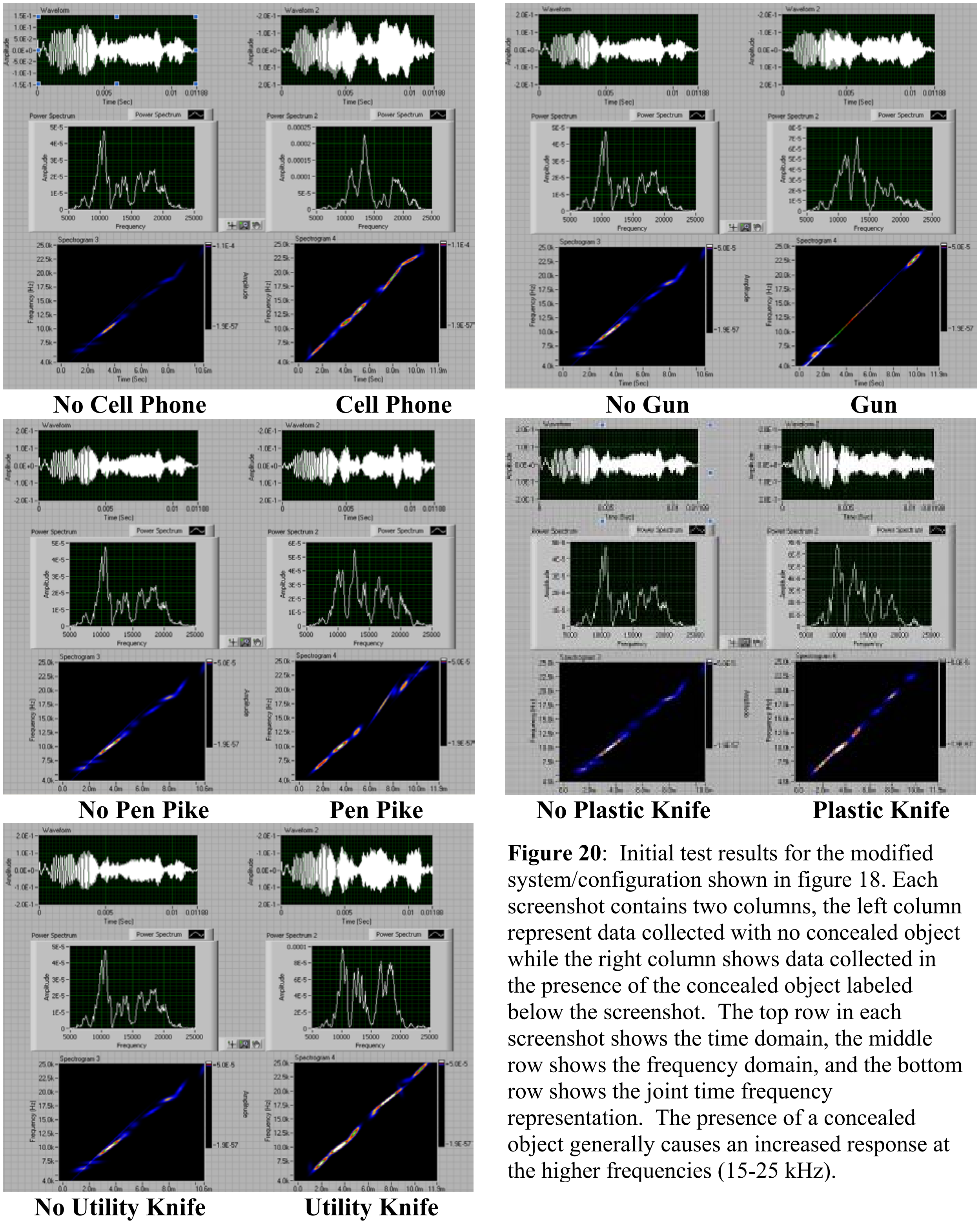

Figure 20: Initial test results for the modified system/configuration shown in figure 18. Each screenshot contains two columns, the left column represent data collected with no concealed object while the right column shows data collected in the presence of the concealed object labeled below the screenshot. The top row in each screenshot shows the time domain, the middle row shows the frequency domain, and the bottom row shows the joint time frequency representation. The presence of a concealed object generally causes an increased response at the higher frequencies (15-25 kHz).

As shown in Figure 19, the initial testing utilized fabric that was stretched uniformly over the tissue simulant with no wrinkles or folds. This configuration is appropriate for initial testing but is not representative of practical situations. As a result, variation in the fabric state was investigated to determine its effect on signal characteristics. The configuration showing the fabric states tested is shown in Figure 21. The results of those tests are shown in Figure 22.

Figure 21: Photograph showing the wrinkled fabric used to test more "natural" fabric states that would be encountered in more practical applications. Compare this with the configuration shown in figure 18. The results of the tests under this configuration are shown in figure 22.

In comparing results from figures 19 and 21 one can see large variations in characteristics signals both with and without concealed objects. As a result, the development of a concealed object signature would prove extremely difficult given so much variation between signals. The source of this variation is mainly caused by the interaction of sound energy with surface of the fabric. Although the source has been placed such that the generated acoustic waves impinge on the fabric at oblique incidence, the receiver microphone is normal to the surface and positioned such that it records a significant amount of that scattered energy from the fabric surface.

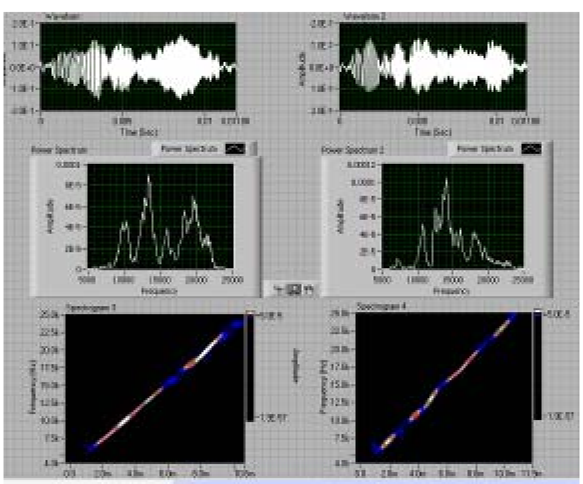

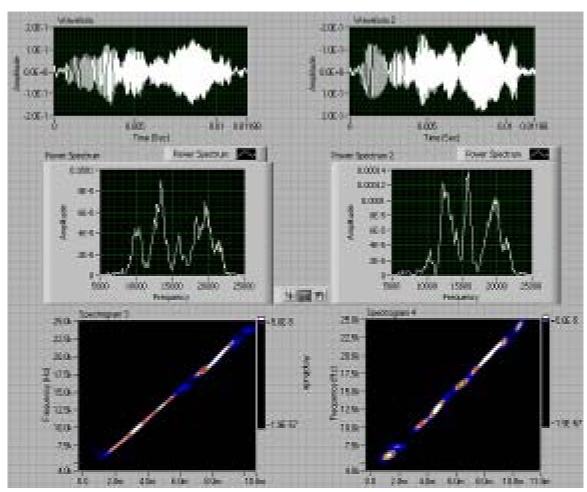

No Cell Phone **Cell Phone** **No Gun** **Gun**

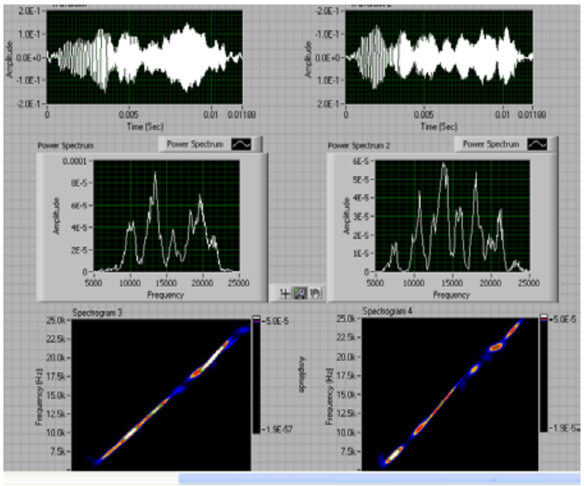

No Pen Pike **Pen Pike**

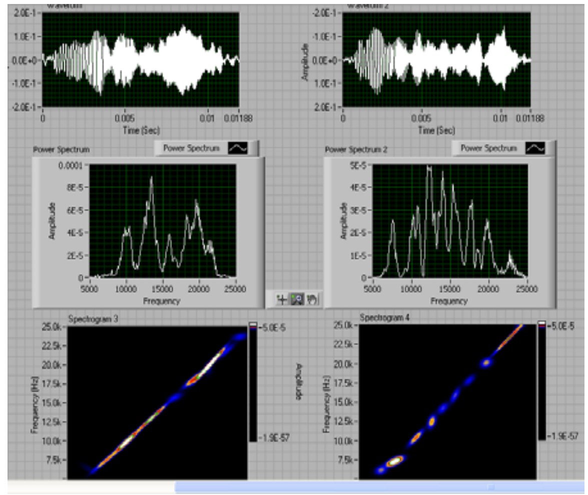

No Plastic Knife **Plastic Knife**

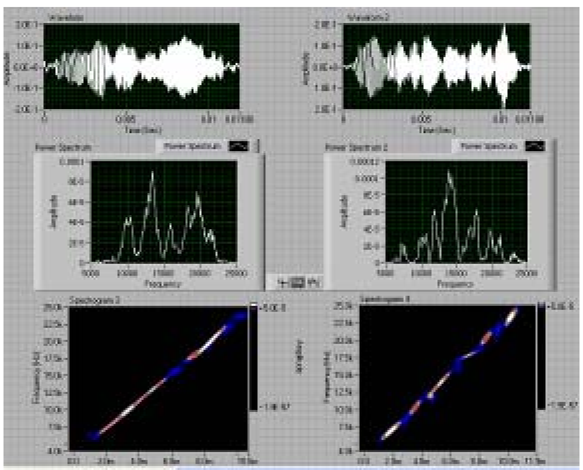

No Utility Knife **Utility Knife**

Figure 22: Test results for the modified system/configuration shown in Figure 21. Each screenshot contains two columns, the left column represent data collected with no concealed object while the right column shows data collected in the presence of the concealed object labeled below the screenshot. The top row in each screenshot shows the time domain, the middle row shows the frequency domain, and the bottom row shows the joint time frequency representation. Although the data with and without concealed objects shows differences, there is a significant variation between this data and the data shown in Figure 20.

To overcome issues associated with the scattered energy from the fabric surface, the microphone receiver was placed within the transmitter array and the incidence angle was greatly increased. There are several benefits to this configuration. First, the greater angle and placement of the microphone helps to eliminate the effects associated with scattered energy from the fabric surface. Secondly, the larger incidence angle allows the system to be much closer to the subject (approximately 5-8”) while maintaining a reasonable path between transmitter and subject (approximately 12-15”). This extra distance helps promote the generation of the nonlinear acoustic signal. A photograph of this new setup is shown in Figure 23. Notice the setup has also graduated from a plain fabric to a standard issue prison jumpsuit, graciously lent to Luna by John Kuplinski, Superintendent of the Virginia Peninsula Regional Jail. In order to keep the development effort on schedule, optimization efforts along with the advancement toward more practical inspection scenarios moved forward in parallel.

Figure 23: Photograph of the current configuration including: increased incidence angle, incorporation of microphone (silver) with the transmitters (white) and the inclusion of a standard VPRJ prison jumpsuit.

Initially testing with the current configuration confirmed the earlier supposed benefits of eliminating effects from fabric surface scattered energy on the received signal. This configuration also helped define a characteristic signature in the signal processing that could be incorporated into the detection algorithm. The suite of concealed objects considered for this testing was updated based on inputs from corrections officials discussed under task 1. The current list of concealed objects under test include: plastic knife, gun, cell phone, paper currency, and a pen-pike. Photograph examples of test setups for some of these objects are shown in Figure 24.

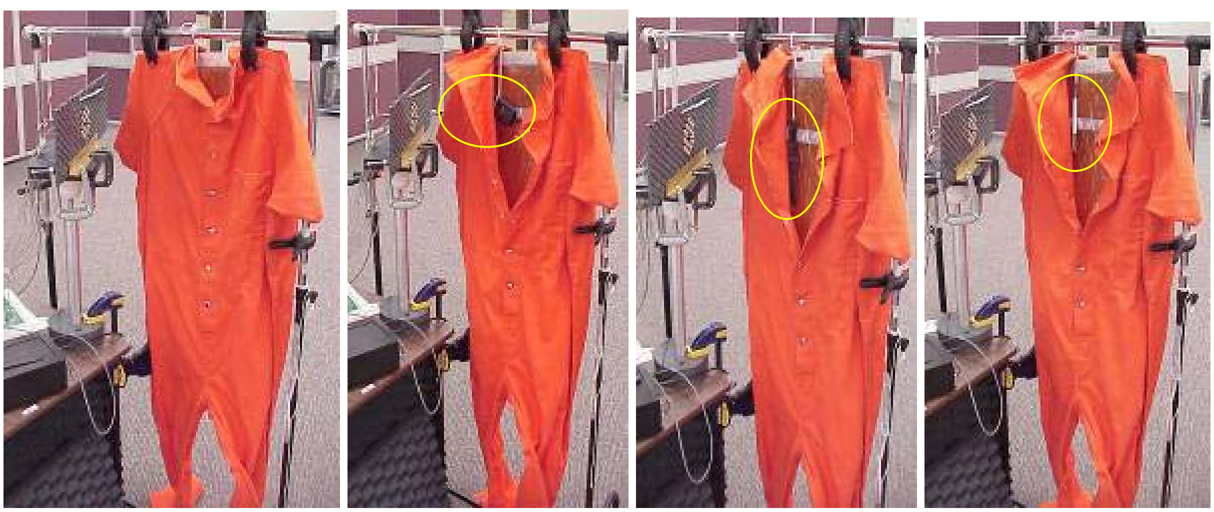

(a) (b) (c) (d)

Figure 24: (a) Photographs showing concealed object configurations containing (b) cell phone, (c) plastic knife, and (d)pen pike. The tests were conducted under a scenario shown in the left most photograph. The other photographs are unbuttoned to show the location of the objects.

Test results for the configuration shown in Figure 24 are shown in Figure 25. Note that these screen shots only include time domain and joint time frequency domain representations of the data. During this round of testing, the algorithm was also pruned to remove much of the peripheral calculations that are not vital to the system's operation but were useful in its development. The motivation was to reduce the computational expense and increase the processing speed in anticipation of moving toward scanning functionality. Part of this pruning included the removal of the frequency domain processing and data representation since it is not capable of representing the time at which certain frequency responses are recorded. It is this time dependence that is critical for proper signal classification.

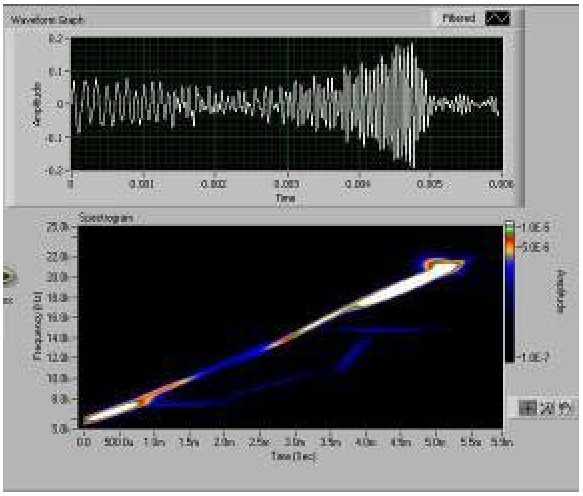

No Cell Phone

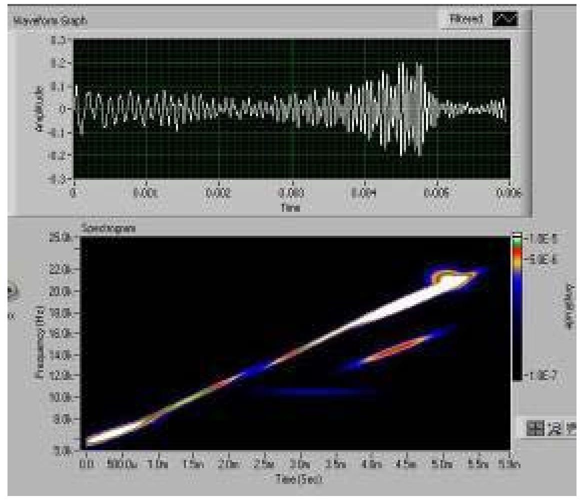

Cell Phone

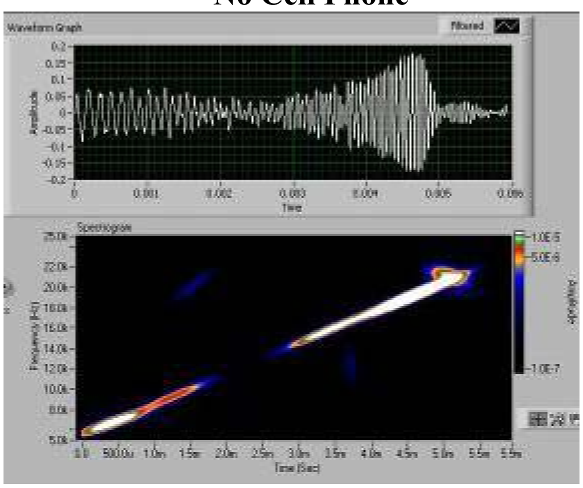

No Gun

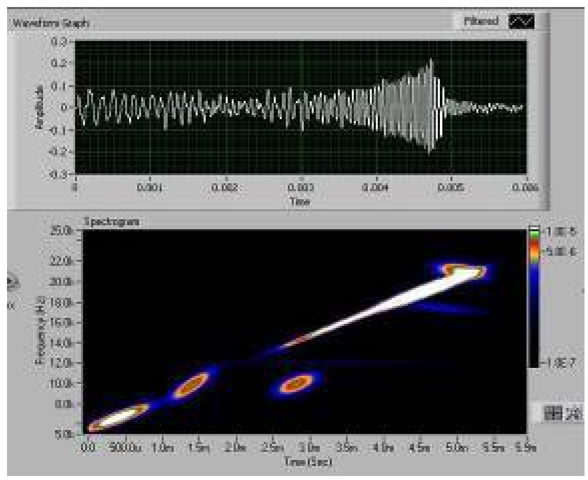

Gun

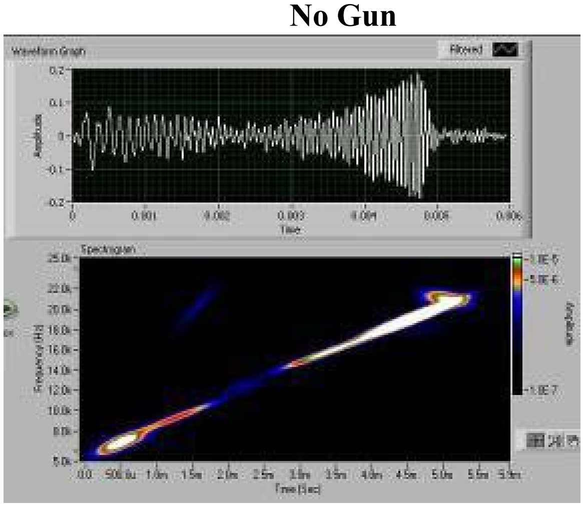

No Plastic Knife

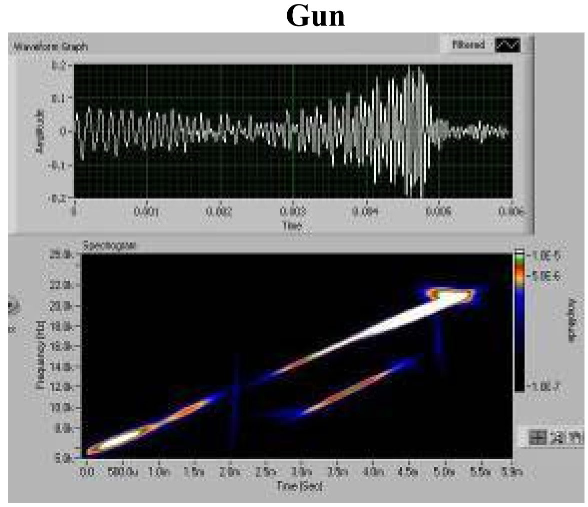

Plastic Knife

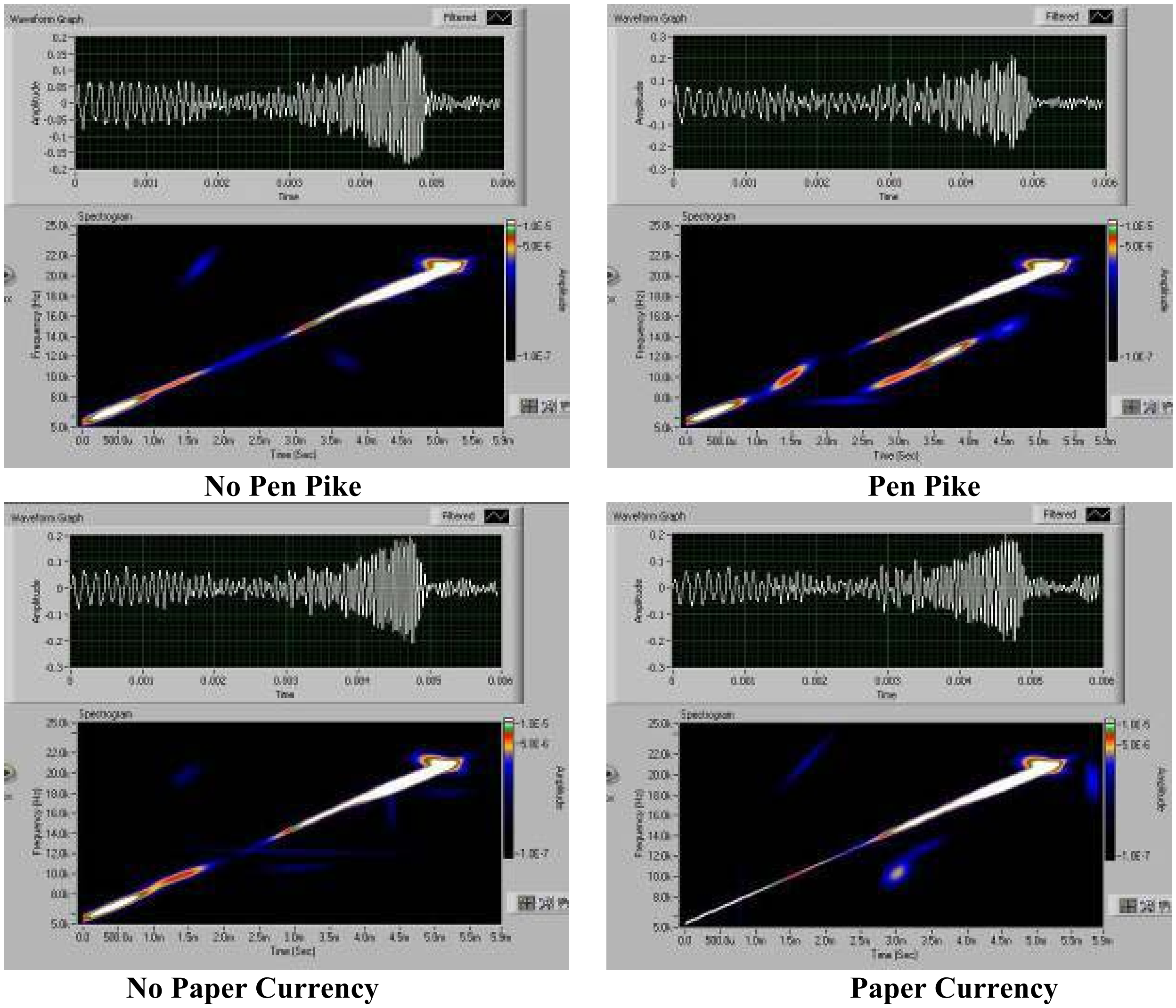

Figure 25: Test results for configuration shown in figure 8 including the time domain and joint frequency representation of the data. Data on the left column was taken with no concealed object while data on the right shows data for scenarios where the labeled concealed object was present. The joint time frequency representation showed a consistent response to a concealed object identified by strong signals below the main diagonal.

The data shown in Figure 25 shows a clear and consistent signature associated with the presence of a concealed object. This signature is the presence of signals below the main diagonal on the joint time frequency representation. The bright colored spots are an indication of the amplitude of that particular frequency (identified by the vertical y-axis) at that particular time (identified by the horizontal y-axis). The bright spots along the main diagonal represent energy that propagates directly from the transmitter to the microphone. When this acoustic energy impinges on the jumpsuit with only ballistics gel beneath it, that energy is reflected off and scattered with no energy returning to the microphone. However, when an object is present, that nonlinear acoustic energy will interact with the tissue simulant ballistics material, resonate portions of the object or cavities in the object, and reflect back to the microphone. It is those interactions that are represented by bright spots beneath the main diagonal.

Using signatures below the main diagonal and the configuration shown in Figure 24, a series of "semi-blind" detection tests were conducted with the aforementioned concealed objects to evaluate the systems sensitivity and false positive rate. The "semi-blind" tests involved capturing signals while repeatedly concealing objects within the acoustic path and removing them. The test was semi blind in that the orientation or placement of the object was not optimized in any way nor was it confirmed that the object was actually in the acoustic path. The results of these tests are shown in Table VII. The detection results and false positive rates show promise for this more finalized configuration. The detection classification in this exercise was based on visual identification of signals below the main diagonal. The development of a numerical detection algorithm was then completed. This algorithm includes thresholding that helps reduce false positive detections.

This algorithm, which ultimately would be included via onboard processing within the handheld detector on the final device, would be the root of triggering for the acoustic portion of the WANDD. Threshold limits can be defined for signals occurring below the main diagonal. When those threshold values are exceeded the algorithm will classify that capture as detecting the presence of a concealed object and a user alert will be triggered either in the form of a light or an alarm located on the handheld device. The position and amplitude of the off diagonal signals would also be compared with a database of signatures from known objects such that the device provides a probabilistic classification capability.

Table VII: "Semi-blind" test results for evaluating sensitivity and false positive rates. The two plastic knife listings represent different orientations of the same object

Concealed Item	Detected (%)	False Positives (%)
Cell Phone	80.0%	10.0%
Gun	100.0%	0.0%
Money	95.0%	0.0%
Pen/Pike	100.0%	0.0%
Plastic Knife 1	100.0%	0.0%
Plastic Knife 2	97.5%	20.0%

This task has been nearly completed during the current reporting period. Remaining optimization efforts are focused on the finalization/implementation of the detection algorithm, excitation signal, and physical parameters that relate to the acoustic system's integration with the Adams Metal detector. These efforts are discussed in more detail under Task 4.

d. Task 4: WANDD integration with Adams Metal Detector

The conceptual design for the detection system of figure 26 shows Luna's initial design for integrating the acoustic and metal detection portion of the ultimate handheld device. Once the first laboratory breadboard was fabricated (as described in Task 2), tests were conducted which integrated the two systems. A separation of approximately 6-8" is required to eliminate cross talk between the two systems. This cross-talk consists of the metal detector picking up the metal associated with the electronics and transducers of the acoustic system. Two solutions to this problem are being considered. The first solution is to isolate the two systems from one another. This requires that they be offset by approximately 6-8". An initial conceptual drawing of this multi-sensor head configuration is shown in figure 27.

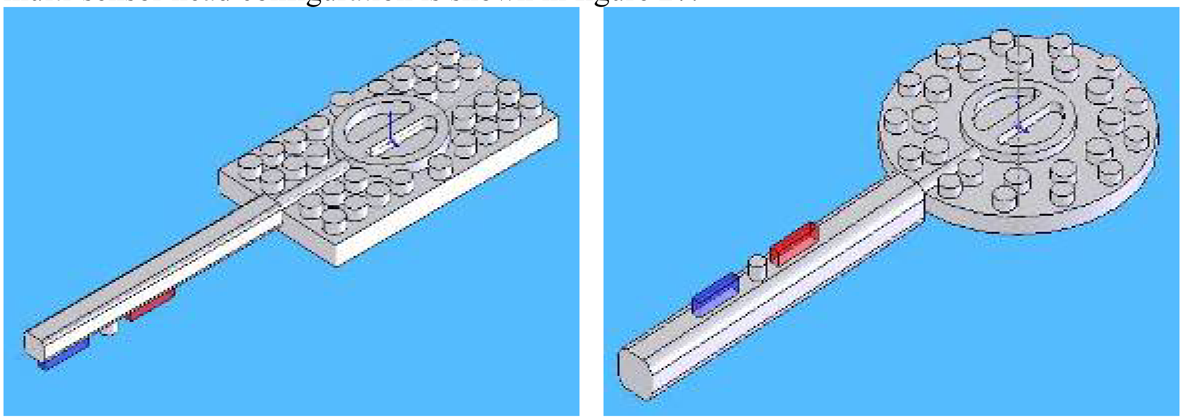

Figure 26: Conceptual drawings for integrating the acoustic transducers (small cylinders) with the Adams metal detector (in the center of both sensing heads).

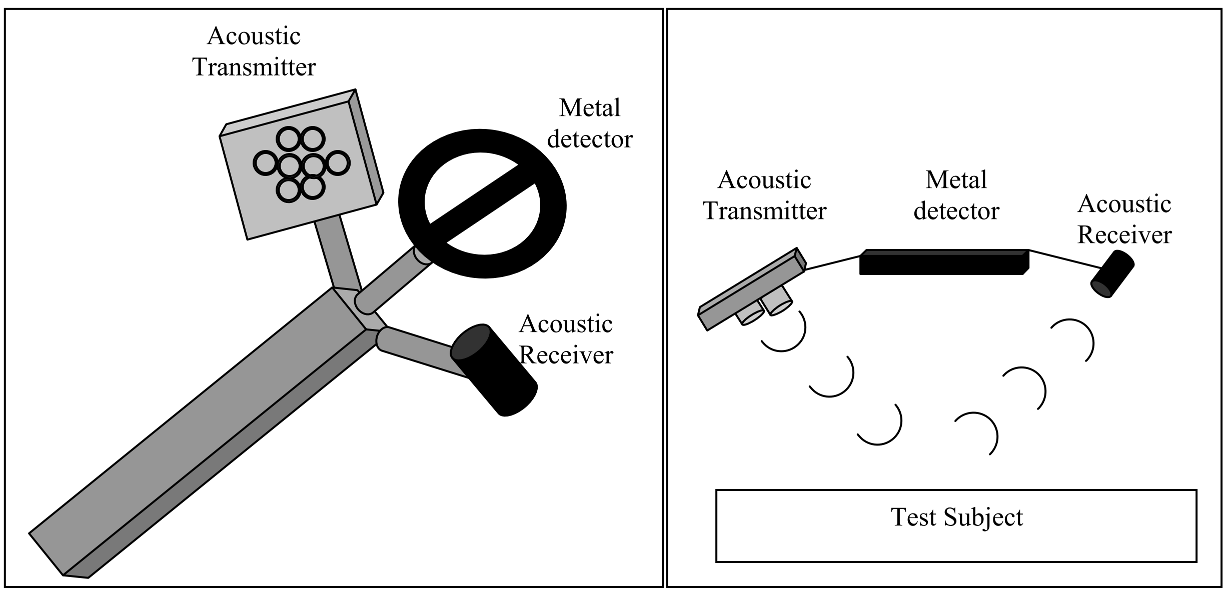

Figure 27: Conceptual design for the multiple sensor head configuration. This configuration will help eliminate the cross talk between acoustic and metal detection units. The angling of the acoustic transmitter and receiver may also help remove specular reflections from the fabric of the test subject.

A second configuration would mimic those shown in figure 26. This design would require a significant reduction in the metal content near the metal detection sensor head. In the final prototype, the electronics will more than likely be moved into the handle. A sufficient spacer between the sensor head and handle will help to ensure that these electronics do not interfere with the metal detection. The transducer models initially tested are available in plastic housings.

It was also conceivable that the number of transducers could be reduced from the original 19. This would have resulted in significant reduction of metal content in and around the Adam's unit. Although this represented initial concept configurations another design was chosen and used for the proof-of-concept system.

The general design of the integrated system has been completed based on the efforts under the previous task. The acoustic portion of the handheld unit will be contained in an assembly that is fixed onto the bottom portion of the Metal Detector. The angular offset of this assembly is such that the acoustic beam will interrogate the same portion of the subject as the metal detector. A mockup of this assembly was fabricated to finalize form factors and positioning. Once finalized, a more permanent fixture will be fabricated as per Task 5.

Two strategies were initially implemented for integration of detection indicators. The metal detector uses two indicators to signify the detection of a metal object. The first is red light on the detector itself and the second is an audible tone. In its current state, that audible tone is in the frequency range of operation of the nonlinear acoustic signal and interferes with its operation. The speaker for that audio output was disabled though the output signal has been fed into the laptop controlling the acoustic portion of the device and a metal detection indicator has been included in the acoustic detection algorithm. This represents the first integration of detection indicators. The second and perhaps more pertinent integration involved an LED indicator for acoustic detection incorporated near the current metal detector light. This provides the operator with a capability to easily identify and discriminate the detection modalities of the device. It was finally decided that integration of the detection indication within the software did not provide added value. The operator would have to continually look back to the laptop screen to confirm detection by the acoustic portion of the device. As this is not ideal, the detection indications were focused on the led indicators on the actual handheld unit.

The general design of the integrated system has been completed based on the efforts under the previous task. The acoustic portion of the handheld unit will be contained in an assembly that is fixed onto the bottom portion of the Metal Detector. The angular offset of this assembly is such that the acoustic beam will interrogate the same portion of the subject as the metal detector. A mockup of this assembly is shown in Figure 28. The housing shown in this figure is the actual housing to be used for the acoustics assembly. This mockup is currently being used to help finalize the angular and linear offsets of the assembly with respect to the metal detector. Once finalized, a more permanent fixture was fabricated as per Task 5.

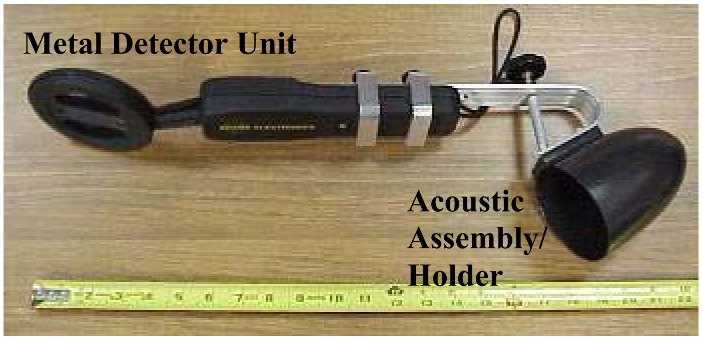

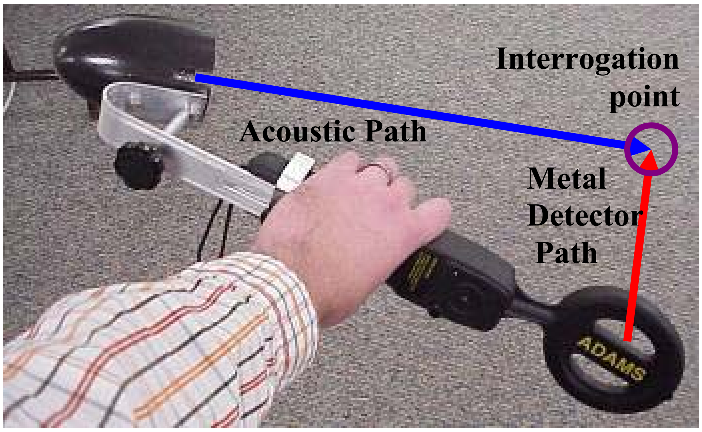

Figure 28: Photographs of the initial mockup being used to optimize the linear and angular offsets of the acoustic assembly with respect to the metal detector unit. A key part of this optimization process is assuring the interrogation point of each detector modality is consistent with one another. This design takes into account survey inputs gathered under task 1 as to the typical metal detector separation from the interrogated subject. This aspect will remain consistent so as to not compromise the functionality of the original metal detector unit.

Currently, two strategies are being implemented for integration of detection indicators. The metal detector uses two indicators to signify the detection of a metal object. The first is red light on the detector itself and the second is an audible tone. In its current state, that audible tone is in the frequency range of operation of the nonlinear acoustic signal and interferes with its operation. The speaker for that audio output will be disabled though the output signal has been fed into the laptop controlling the acoustic portion of the device and a metal detection indicator has been included in the acoustic detection algorithm. This represents the first integration of detection indicators. The second and perhaps more pertinent integration will involve an LED indicator for acoustic detection to be incorporated near the current metal detector light. This will provide the operator with a capability to easily identify and discriminate the detection modalities of the device.

e. Task 5: Build Prototype and Test Matrix

The initial focus of this task was the design and fabrication of the final proof of concept system. First, the array holder and assembly were completed along with the distribution circuit board to power each of the transmitters. The initial mockup for the assembly was shown in Figure 27. Photographs of these sub-components are shown in Figure 28. Next, efforts were focused on building the appropriate elements of the power supply and amplification subsystems. Once the offsets mentioned under task 4 were appropriately defined, the final assembly fabrication was completed. Completion of the electronics subsystems and power supplies finalized the fabrication of the system.

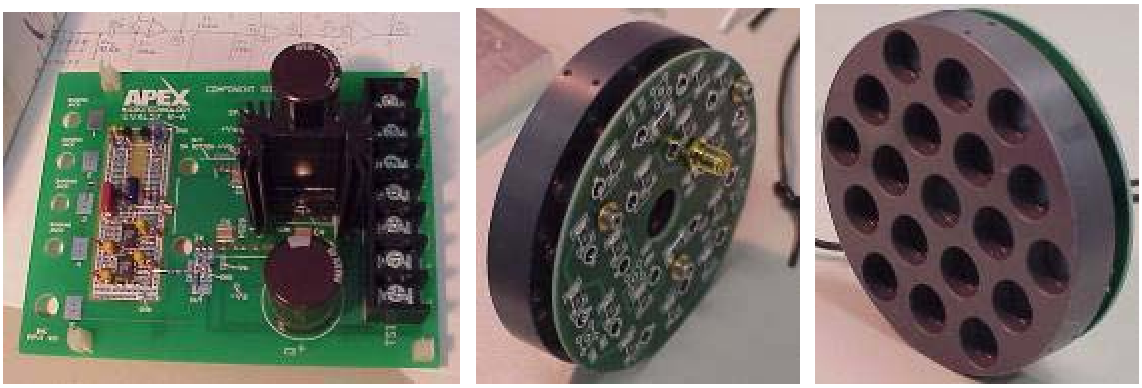

Figure 29: Photographs of several device sub-components currently being fabricated (from left to right) amplification stage, distribution board for the transmitter array, and the front side of the distribution board showing the transmitter/microphone holders to be mounted in the assembly shown in Figure 28.

The electronics requirements for this project changed drastically during the course of the project, particularly after realizing the need to switch from 40 kHz to 210 kHz transducers. The voltage drive requirement for the 210 kHz transducer was 80V peak to peak (Vpp) whereas the 40 kHz transducers only require 40 Vpp. With the first prototype board, we were able to modify the output stage to generate a higher output voltage from the 40Vpp by adding a step-up transformer with a voltage step-up of 1 to 3.

The electronic requirements are different than those posed by a standard audio amplifier for the home, audio or portable MP3 player. One of the chief requirements was to operate with the 190 kHz-220 kHz bandwidth with an input signal that was a relatively fast frequency chirp covering a span of 5ms to 20 ms. The use of the chirp signal prevented the use of a highly resonant impedance matching circuit such as those on the output of most switching amplifiers. The amplifier also had to be a low impedance output linear amplifier to eliminate spurious reflections from modifying the output signal. As part of the electronics development, we did try to drive the transducers with a square wave chirp as opposed to a sine wave chirp signal but found that the sine wave chirp produced more reproducible results and a better excitation signal. At this stage of the WANDD development, we did not want the electronics to limit the frequency, drive level or duration of the transmitted signal. Once the key features in the return signal were identified, the frequency range could be limited to allow smaller amplifier electronics.

We first considered modifying the first prototype board by replacing the original PA09 amplifier with a PA98 amplifier. The maximum voltage on the current PA09 amplifier is +/- 40 V and the maximum voltage on the PA98 amplifier is +/-75V. A single PA98 is limited in its output current to 200mA and each of the transducers had an impedance of 200 Ohms. This results in a current draw of 160 mA per transducer or a total of 6 amperes for the 19 transducer array with a resulting impedance of 12 Ohms. This exceeds the current capabilities and power capabilities of a single standard power amplifier. Upon further reflection at the duty cycles required for faster scanning, we first considered using a PA98 amplifier to generate the proper voltage signal and to follow it by five MOSFET source followers as low impedance drivers to drive five of the transducers. By using source followers, they have a wider frequency bandwidth and with a gain of 1, only serve as current sources. The problem with the source followers is to get the heat out of the packages at the duty cycles (5% to 10%) required for fast scanning. However, we were able to speed up the electronics development by using the MP111 amplifier from APEX/Cirrus which can handle the large current requirements to drive the full 19 transducers. A schematic of the final amplifier is shown below in Figure 30. This customized approach to developing necessary amplifier stages not only provides the operational characteristics necessary for device operation but provides more control over development and cost in transitioning this device to the next stage.

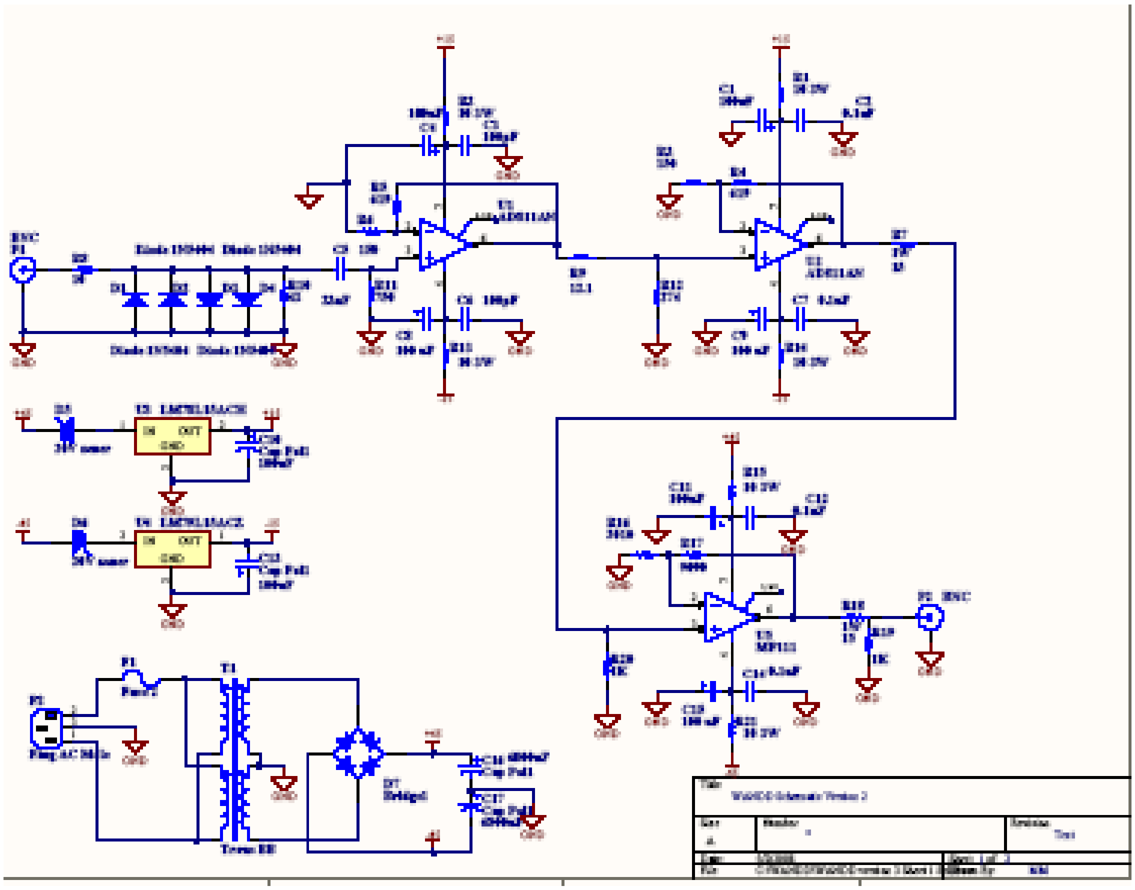

Figure 30: Final design of high power amplifier for 5% duty cycle to drive the 19 element 210kHz transducer array.

A photograph of the final proof of concept device during testing at VPRJ is shown in figure 31. The system consists of an Agilent function generator which produces the tailorable chirp signal used to interrogate the subject. This signal is then amplified through Luna's custom power amplifier previously described. The amplified signal is then sent to the sensor head through umbilical cabling. The amplified chirp signal, via the custom distribution board shown in figure 29, is sent to each of the 19 transmitters. Reception of the non-linear acoustic signals is achieved through a G.R.A.S. measurement microphone and preamp assembly located at the center of the acoustic sensor head. The signal is then sent through a custom receiver gain stage and digitized by a National Instruments Data Acquisition box with USB connectivity back to the control laptop. This laptop is used to define the initial chirp characteristics, control the device operation, capture/store data, and complete all necessary post processing. Two other custom components are included one of which, communicates back to a newly installed LED indicator on the Metal detector head used to indicate an acoustically detected event to the user. A second component currently in place takes the Metal detector output from the device back to the laptop for incorporation with the control software.

Figure 31: Photographs of the WANDD proof-of-concept device during testing at the Virginia Peninsula Regional Jail (VPRJ). Note the cart is used to house all of the electronic components along with the control laptop. The handheld device connects to all necessary electronics through a single cable bundle.

Evaluation of the proof-of-concept device was conducted both at Luna's facility and VPRJ. A systematic test matrix implemented at Luna's facility was designed. The test conditions and variables included in the test matrix are shown in table VIII. The test matrix was designed such that an overall assessment of the instrument could be made as well as independent test subsets to provide more detailed analysis of the devices strengths and weaknesses.

Table VIII. Conditions and Settings included in Test Matrix Evaluation

Subject Condition 1	*White VPRJ Suit Orange VPRJ Suit Casual Clothes (note type)*
Subject Condition 2	*Male Female*
Device Setting 1	*Cursors 1-4: Frequency and Time*
Test Condition 1	*Plastic Knife Sm. Handgun Pen Pike Cell Phone Credit card None*
Test Condition 2	*Chest Stomach Hip Side pocket Ankle Knee Side thigh Back Front shirt pocket*

f. Task 6: Test Prototype

Approximately 20 individuals were scanned as part of the test matrix evaluation including more than 50 qualitative and quantitative test sets. Overall evaluations were based on more than 2000 samples where both inmate and visitor scenarios were included (as shown by Subject Condition 1 in Table VIII). Photographs of "visitor scenarios" are shown in figure 32. Scenarios representing inmate scenarios are shown in figure 33. In both figures, the areas where items were concealed are shown. Differences in location were considered as a result of the availability to conceal items given the particular clothing scenario. For instance, the orange VPRJ suit has no side pockets but does contain a front chest pocket. In the case of the casual clothed individuals, the plastic knife was used as the concealed weapon while in the case of the VPRJ suits, several concealed items were considered including: the plastic knife, pen pike, small handgun, currency, credit card, and cell phone. Photographs of these items are shown in figure 34.

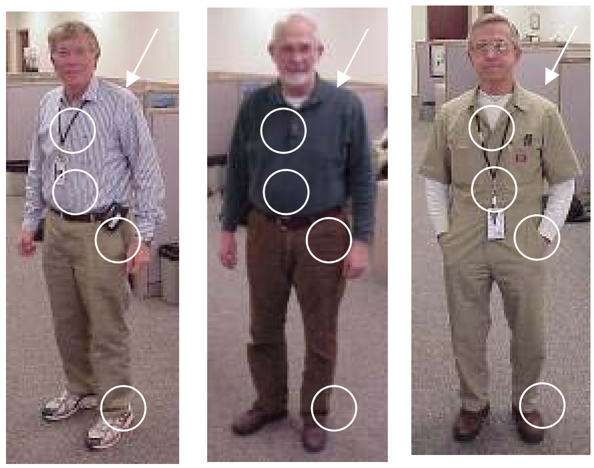

(a) (b) (c)

Figure 32: Individuals included in the test matrix evaluation including highlighted areas where items were concealed.

(a) (b)

Figure 33: Scenarios used to evaluate concealed object detection in the VPRJ prison suits.

Figure 34: Objects used in the test matrix evaluation. The plastic knife on the left was used for the casual clothes evaluation

The results of these test matrix evaluations are shown in Table IX. Shown are the overall results along with subsets of individual scenarios. The first scenario represents lighter casual clothes. This subset excludes those individuals wearing heavier clothes such as winter knit collared shirts, overalls, and sweaters. Examples of these scenarios are shown in figure 31 b and c. The other two subsets indicate the two prison jumpsuits lent to us by the Virginia Peninsula Regional Jail as shown in figure 33.

Table IX: Test matrix results including detector efficiency and false positive rates

Test Matrix Scenario	Detection Efficiency (%)	False Positive (%)
Initial Laboratory Test	95.4	5.0
Overall	66.9	32.3
Lighter Casual Clothes	87.4	56.9
White VPRJ Suit	75.9	46.7
Orange VPRJ Suit	57.6	43.1

The results shown in Table IX were determined via Receiver Operating Characteristic (ROC) analysis described later in the report. The feature used for this analysis is the sum of amplitudes contained in the user identified areas indicated in figure 35 with the purple and green squares. Figure 35a represents a scenario with no concealed object present whereas figure 35b is characteristic of the presence of a concealed object.

The initial laboratory assessment consisted of a flat ballistics gel tissue simulant and Orange VPRJ suit (as shown in figure 23). The detector efficiency and false positives for this scenario demonstrate the proof-of-concept of the systems modality. The overall assessment is an inclusion of all data taken during the final test matrix. This demonstrates the system capability in real world scenario in its current state. It is also important to note that this includes all scenarios tested including all clothing types and all concealed objects. A subset of data was taken for “lighter clothes” scenarios. The purpose of this subset was to confirm the device’s enhanced detection efficiency as a result of lighter clothing. This helped confirm that further increase in sound pressure would help increase the detector efficiency particularly in the presence of heavier clothes. This aspect is further confirmed with the detection efficiency of the VPRJ suits. A higher detection efficiency was demonstrated with the white VPRJ suit, which is a thinner fabric than the orange VPRJ suit.

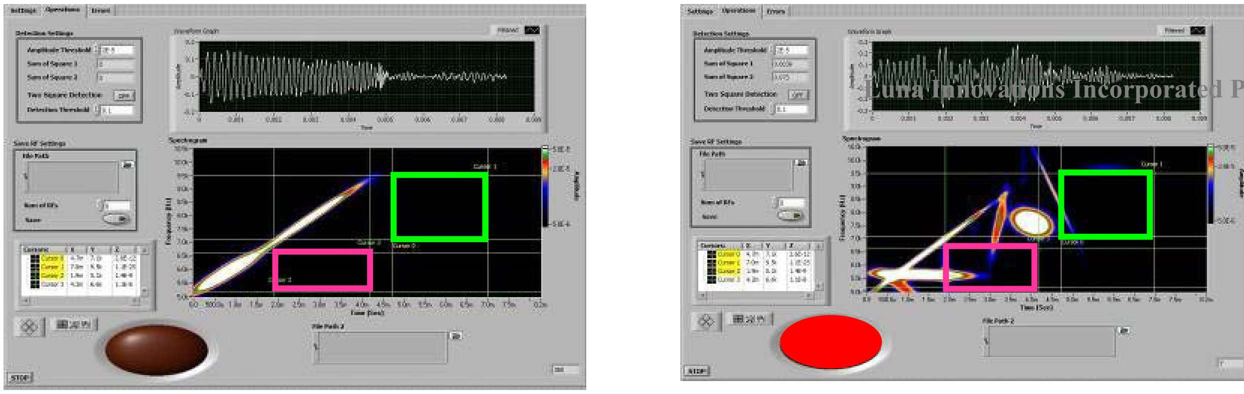

(a) (b)

Figure 35: (a) Representative waveform representing no concealed object and (b) representative waveform in the presence of a concealed object.

The ROC curves for the overall test matrix results and the lighter casual clothes scenario are shown in figure 36. These curves are used for systematic evaluation and provided the basis for the results shown in Table IX. These curves are also used to provide optimal thresholds to be used in triggering the LED indicator on the device handle. The ROC curves were generated via data obtained in the test matrix evaluation. JMP software was used for the analysis.

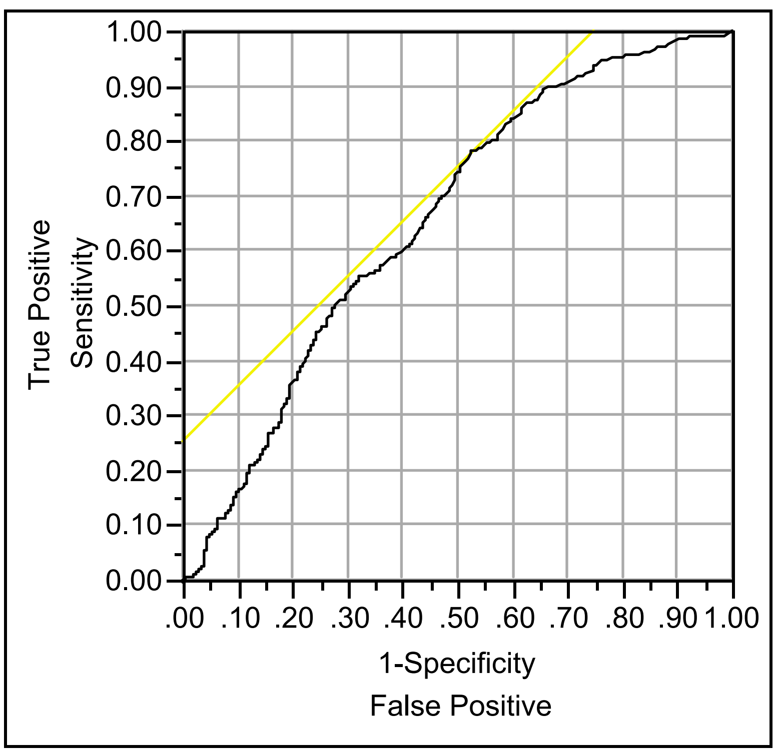

(a)

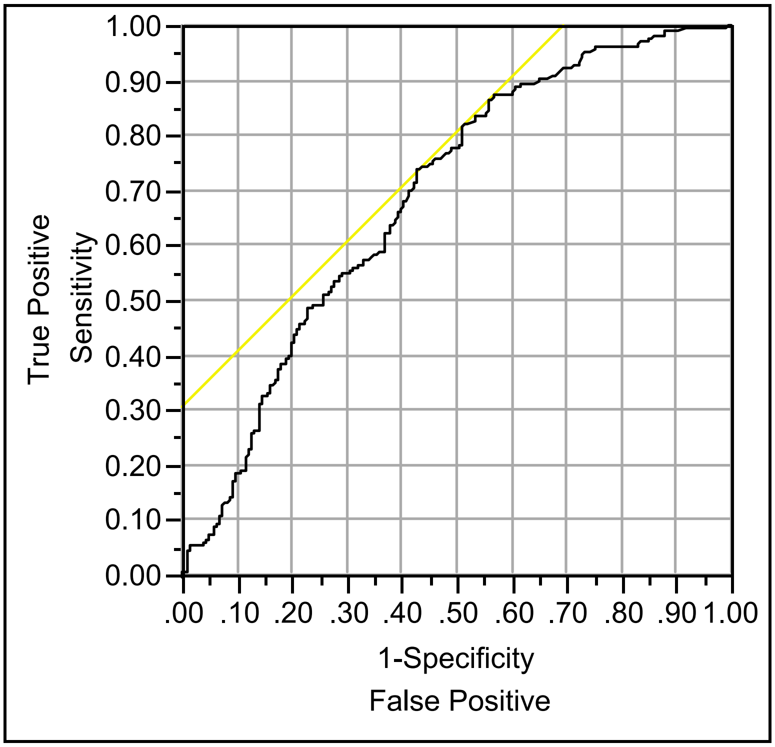

(b)

Figure 36: ROC curves for (a) overall analysis and (b) lighter casual clothes subset.

The nature of the ROC curve is to evaluate a systems sensitivity and selectivity. Sensitivity represents true positives, i.e. situations where hidden objects where correctly identified. Selectivity represents true negatives, i.e. situations where the lack of hidden objects where correctly identified. The curves typically range from a straight line of slope 1 for the worst case to an initial rapidly increasing curve which asymptotically approaches 1 for the best case. The physical interpretation of the latter type of curve is that the sensitivity increases rapidly with little change in false positives.

As previously mentioned, the sum of frequency amplitudes within user identified regions were used as the characteristic feature for detection. The ROC curves in figure 36 are determined by evaluating incremental increases in that threshold value. For instance, the software assigns a threshold value of 0.1. It then compares all data to its known state. In this case, data sets with amplitude higher than 0.1 are labeled as true positives for cases where an object was present and false positives for cases with no object present. Data sets with lower amplitude values than the threshold are false negatives when a hidden object is present and false true negative when no hidden object is present. In order to be consistent across all data subsets, an optimize threshold value of 0.21 (obtained using all data in the test matrix) was used for each analysis. These results were reported in Table IX.

g. Task 7: Deliver to NIJ and provide Technical Support

The details of delivery and support are currently being discussed with NIJ.

h. Task 8: Commercialization Planning and Next Steps

Luna has talked to a number of major national security companies who have expressed interest in this technology. To move to the next level of interest, the TRL of the prototype should be carried to the next level. It is our estimate that we are now at TRL 5. A Phase II from NIJ, perhaps in partnership with a second government office, will enable Luna to invest more development into the analysis software and fine-tuning the hardware bringing the device to a sufficient development level for commercialization.

During the NIJ meeting in Orlando October 24,25, 2007, an interesting discussion arose concerning the market realism of the various developers who were funded by NIJ. Luna had explored that realism earlier in discussions with the Northeast Technology Product Assessment Committee (NTPAC) in their meeting of June 29,30, 2005. Those conversations and subsequent discussions with members of the corrections community helped the Luna project focus on an ultimate cost boundary in the several thousands of dollars, in some volume production.

Therefore it was no surprise that the Luna approach was identified at the Orlando meeting as one of the only talks that addressed the needs of the community as to projected cost targets. Since winning the NIJ Phase I, we have continued to focus on a development that is targeting that price range. The next Phase II funding will permit the technology development and software advancement to reach the technical and design considerations that are needed to move this device to attract funding to commercialize this device.

Extensive consultation with transmitter supplier, Massa Products Corporation, has continued throughout this effort. The consultation with Massa continued on two fronts. The first focus was the technical performance of Massa's suite of transmitters and ultimately the performance and specifications of the currently used transmitters. The second focus was the price point for transmitters at volume levels again to ensure their viability within current market price points for a WANDD-like device. At volume production levels (i.e. 1000+), per unit costs are approximately $20/transmitter (with 19 total transmitters currently). This is reasonable for the transmitter portion of the sensor while maintaining an ultimate price point for the device. With continued Phase II efforts, Luna would sign an NDA with Massa to continue such discussions.

Luna requires a second phase of funding support to mature this technology. Based on the successful tests conducted in this phase, it is clear that the project warrants consideration for continued development. The rate of progress for this phase has been exceptional resulting in a breakthrough technology application and demonstration. It is clear that there have to be improvements in the form-factor of the system and in the false-calls. Based on the findings, we believe both of those goals will be met if funded for the next phase. Improvements in the extraction software along with wireless operation will be part of the next generation development.

IV. Appendix A: Luna's Questionnaire on Contraband Detection

LUNA INNOVATIONS

inspired by ideas . . . driven by markets

July 3, 2007

Dear Requirements Correspondent;

Luna Innovations Incorporated is working under contract with NIJ to develop an enhanced hidden object sensor similar to hand-held metal detectors but with enhanced capabilities.

Our goal is to build a prototype device to be tested in real facilities that may lead to a next generation device for the corrections field. The device under development will detect both metal and plastic objects hidden on a person under clothing.

In this request, we are asking for your help in providing customer feedback to help guide us during the design of the prototype device.

I have enjoyed meeting many of you at various meetings. Mr. Alex Fox has agreed to help distribute this requirements questionnaire to a select group who are likely to respond within three weeks with realistic information.

We thank you in advance in participating in this questionnaire knowing it will help us in the design of the device.

With kind regards;

Joseph Heyman, PhD.
Chief Scientific Officer
heymanj@lunainnovations.com;
757-224-5692

Please send all responses by July 26th to:
Dr. Mike Pedrick
130 Research Drive; Suite 300
Hampton, VA 23666
pedrickm@lunainnovations.com
757-224-5723

Requirements Survey Questions for Corrections Experts:

1. What is a typical/appropriate scan time?

2. What is the distance tolerance in terms of sensor standoff from the subject?

3. Describe the typical operating conditions and environment. Please include information about if the searchers are indoors or outdoors, if moisture or rain is present, if the environment is unusually noisy or loud and other conditions as you see fit.

4. What amount of instrument on-time is appropriate for continuous operation? This can also be defined in terms of duty cycle (i.e. two minutes on/one minute off continuously for eight hours). Given these operation times, what is an acceptable battery lifetime?

5. How rugged should the device be (i.e. resistant to drops)?

6. What is the maximum practical size for the scanning device (Figure 6 below provides some conceptual design sketches for reference)?

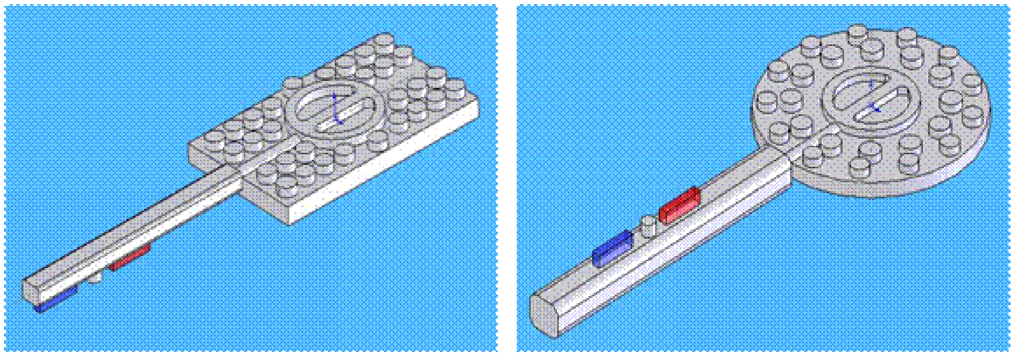

Figure 6. *Conceptual sketches of possible WANDD commercial configurations*

7. What is a realistic upper cost sensitivity for a system that greatly enhances the value of your security checks?

8. In your facility, how many security hand scanners do you currently have on-hand? If you replace these components, how many do you replace in a year?

9. Would you be willing to participate in helping evaluate a new scanner by providing feedback to us after you have been trained and use our system for a trial period?

10. Please describe the type of hidden items you wish to detect. Be as specific in your description as you can such as to the size, material, geometry of the contraband item. Also, how many such items do you confiscate in a year and what is your population? We define contraband as any item you do not permit a person to carry.

11. Please describe the typical clothing of individuals subject to scanning. Include details about the types of fabrics and the number of clothing layers.

12. Where does your population typically hide contraband they carry on their body now? Please be as specific as you can.